



Advanced Laser Doped Solar Cells

Never Stand Still

Faculty of Engineering

School of Photovoltaic & Renewable Energy Engineering

UNSW 22nd May 2014

Brett Hallam



Overview

- Introduction – Laser doping
- Continuous Wave Laser Doping for Deep Junction Formation
- Modelling Diffusion in Laser Doped Regions
- Laser doping from Al_2O_3
- Contacting Buried Layers in Silicon Solar Cells
- Passivation of Laser-Induced Defects



Introduction – Laser Doping



Laser Doping

- Perform diffusion in liquid phase
 - Diffusion coefficients many orders of magnitude higher than in the solid state
- First demonstrated < 1970 [Fairfield 1968]
- Variety of approaches
 - LD from ion implanted dopants or PSG layer
 - SOD layer application
 - Gas immersion laser doping
 - Laser chemical processing

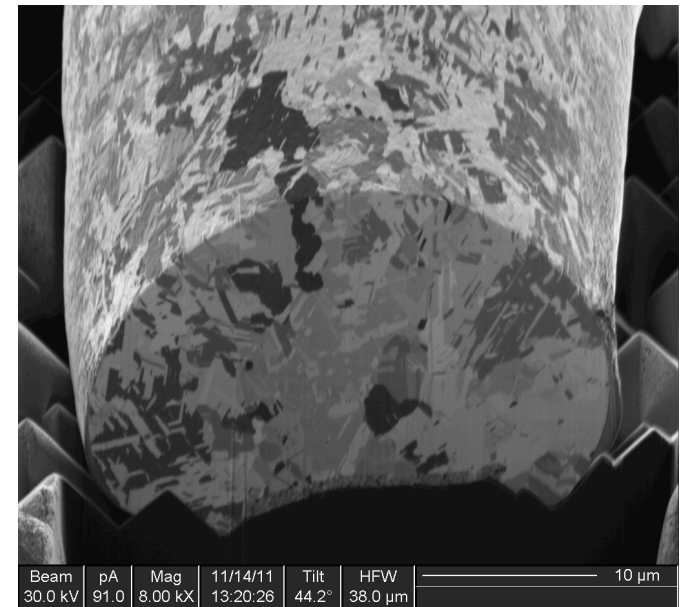
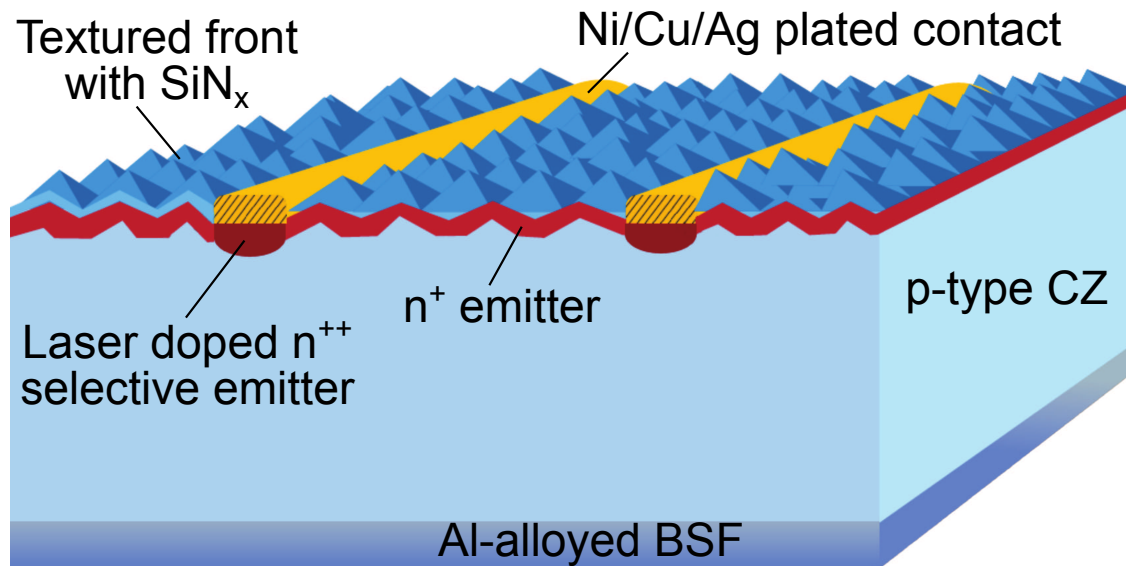
Defect Generation during Laser Doping

- Laser-induced defects have hampered performance of laser doped solar cells
- Defect generation is a complex process dependent on:
 - Orientation of silicon
 - Purity of dopant sources
 - Pulse energy
 - Repetition frequency
 - Dielectric layers
- Avoiding performance degradation
 - Perform laser doping on bare silicon
 - Use an intermediate SiO₂ layer
 - Use continuous wave lasers



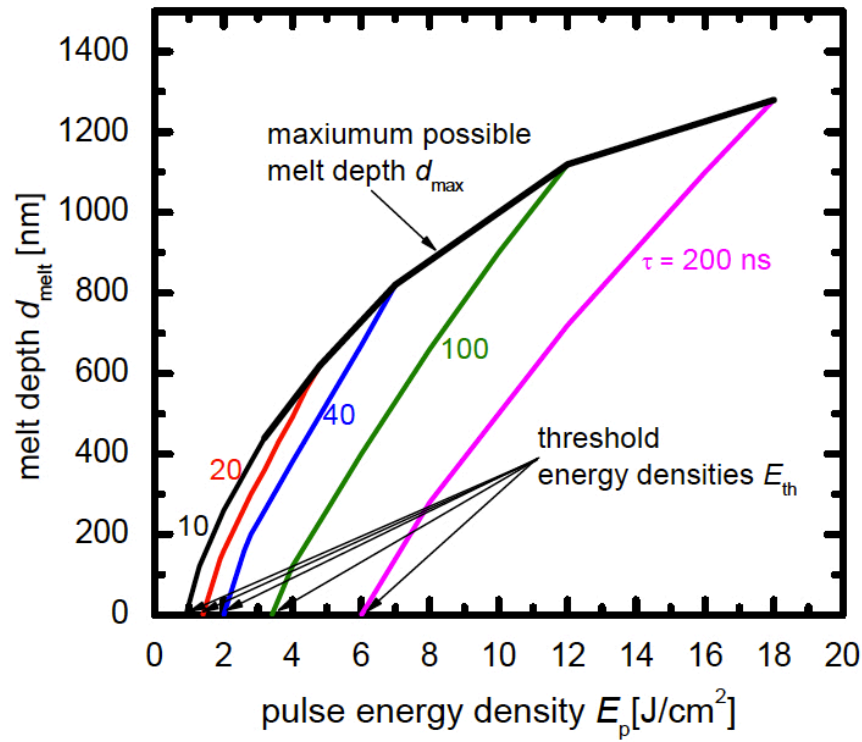
Self-aligned Laser Doped Selective Emitter

- Self-aligned process compatible with light-induced plated contacts [Wenham 1998]
 - Simultaneous opening of dielectric / doping of silicon
 - Contacts $< 30 \mu\text{m}$



Junction Depth Limitations

- Solidification between successive pulses greatly limits junction depths.
- Longer pulses are required to form deep molten regions without ablation of the silicon

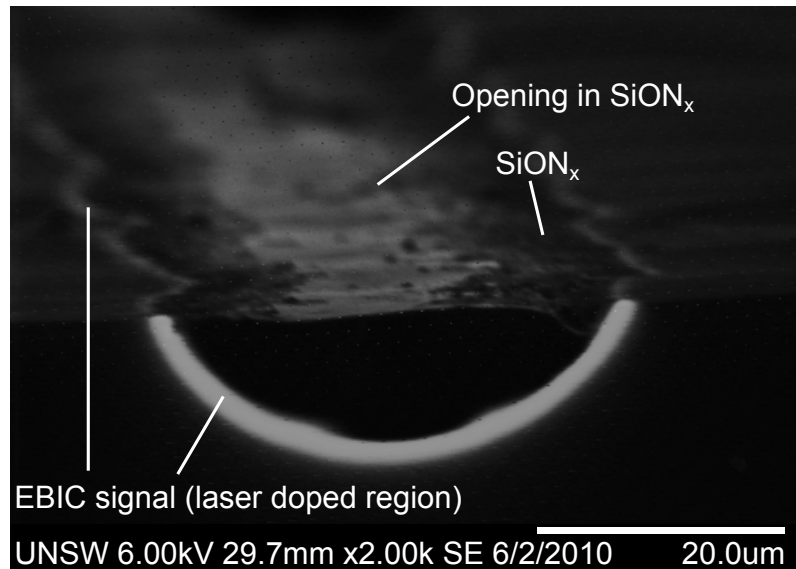


Continuous Wave Laser Doping for Deep Junction Formation

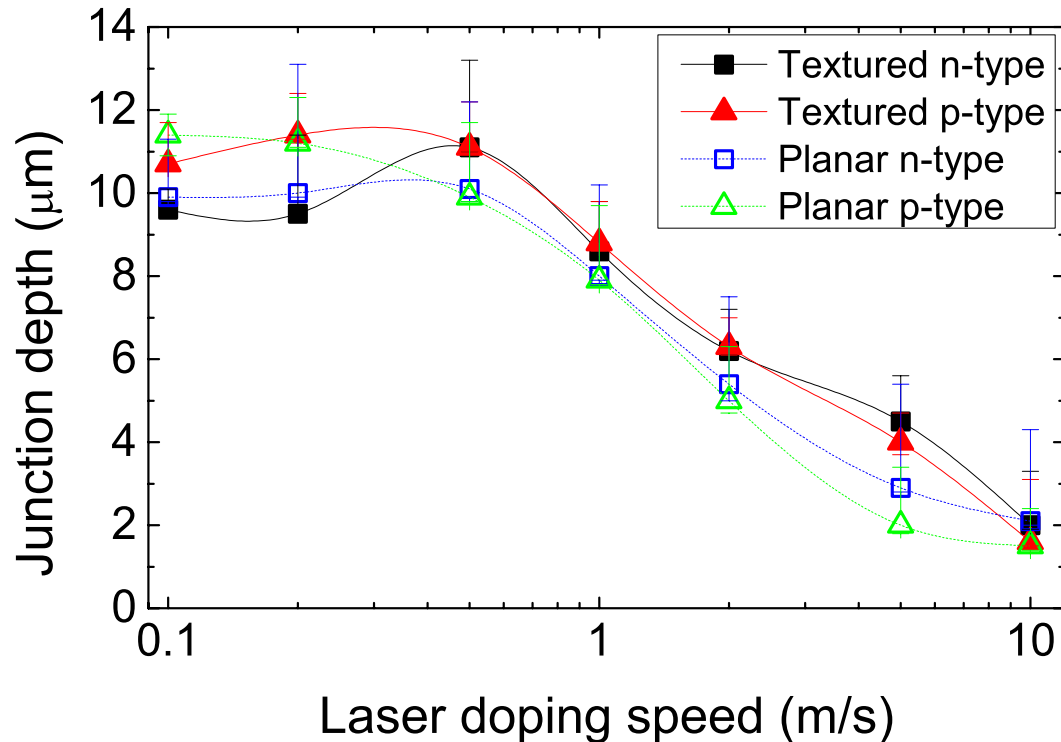


Deep Junction Formation through CW Laser Doping

- CW lasers allow for a deep molten region to form ($> 10 \mu\text{m}$)
 - Silicon remains molten throughout process
- Junction depth can be controlled by processing speed

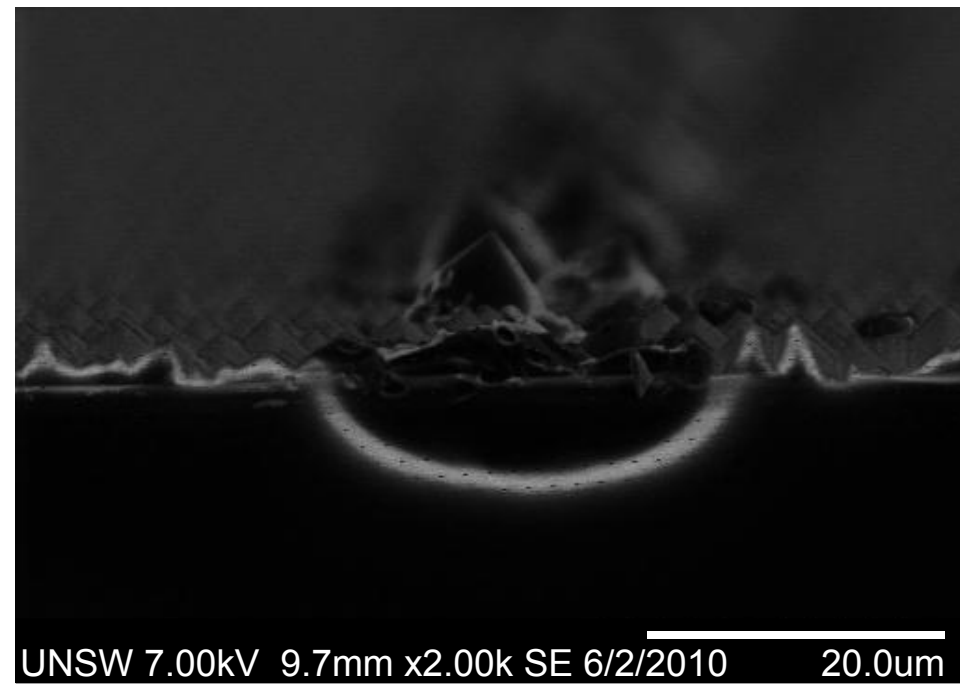
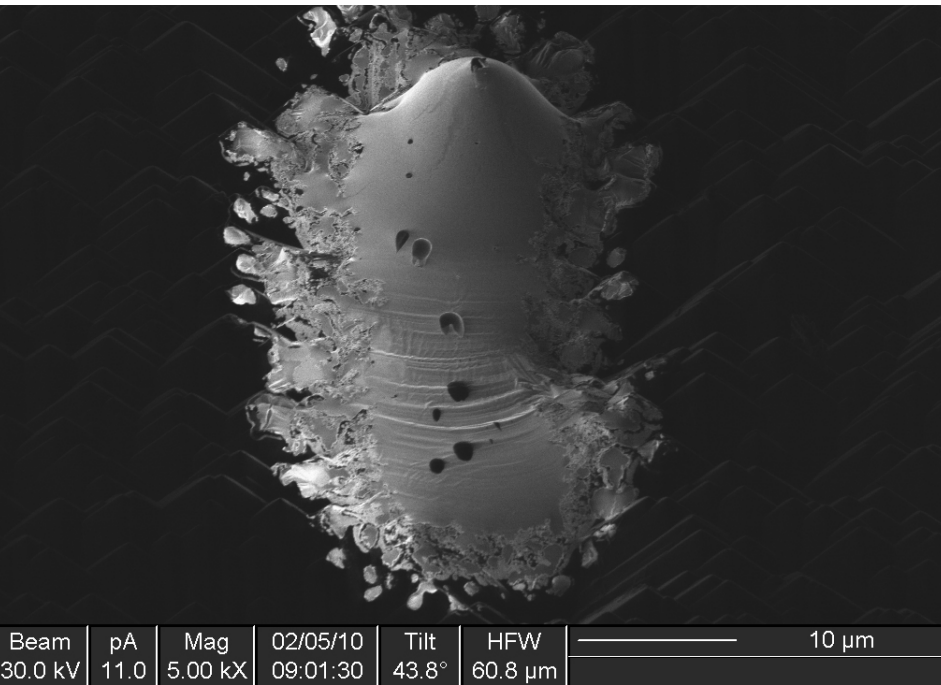


p-type LD on a planar surface (0.2 m/s)



Point Contact Formation

- Point contacts formed using CW laser and physical mask
 - Junction depths over $8\ \mu\text{m}$
 - Small contacts with effective doping

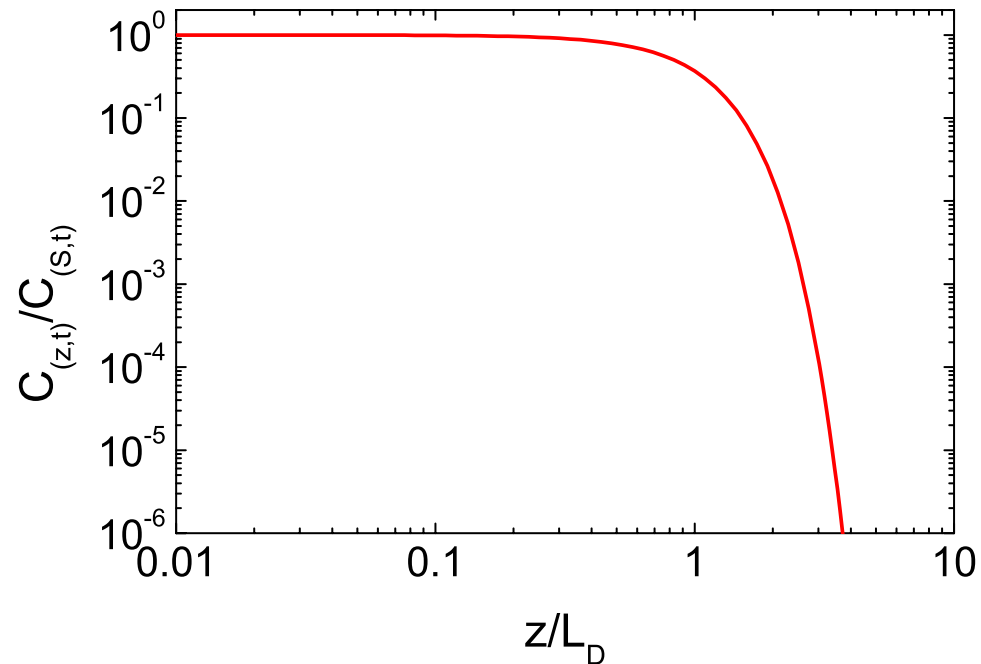
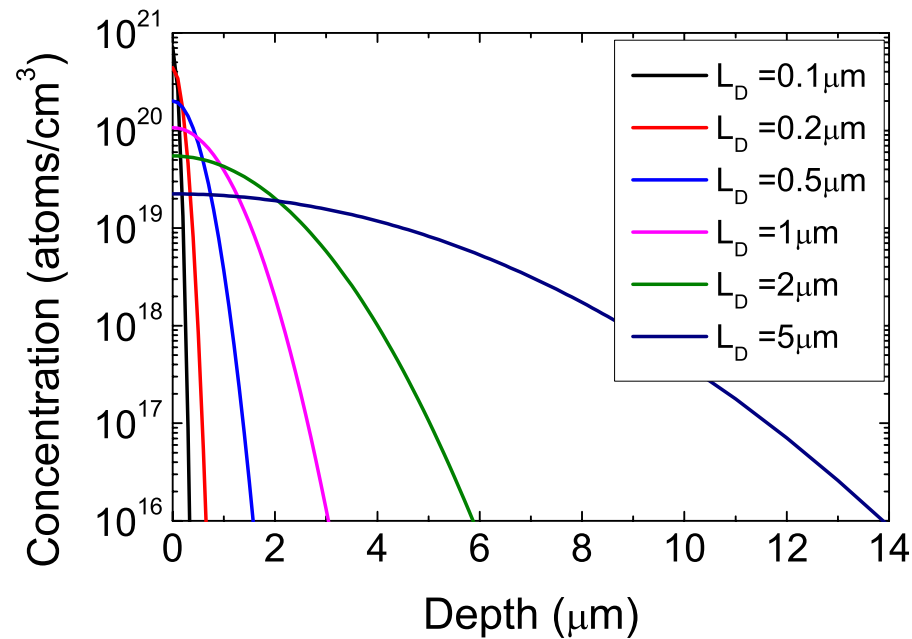


n-type LD on a textured surface (0.5 m/s)

Dopant Profiles in Laser Doped Regions

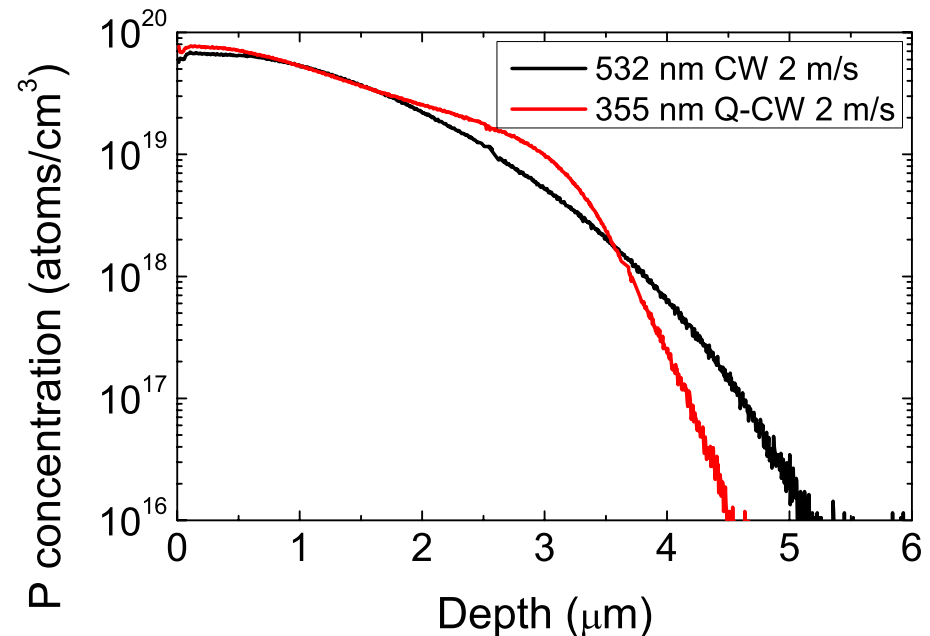
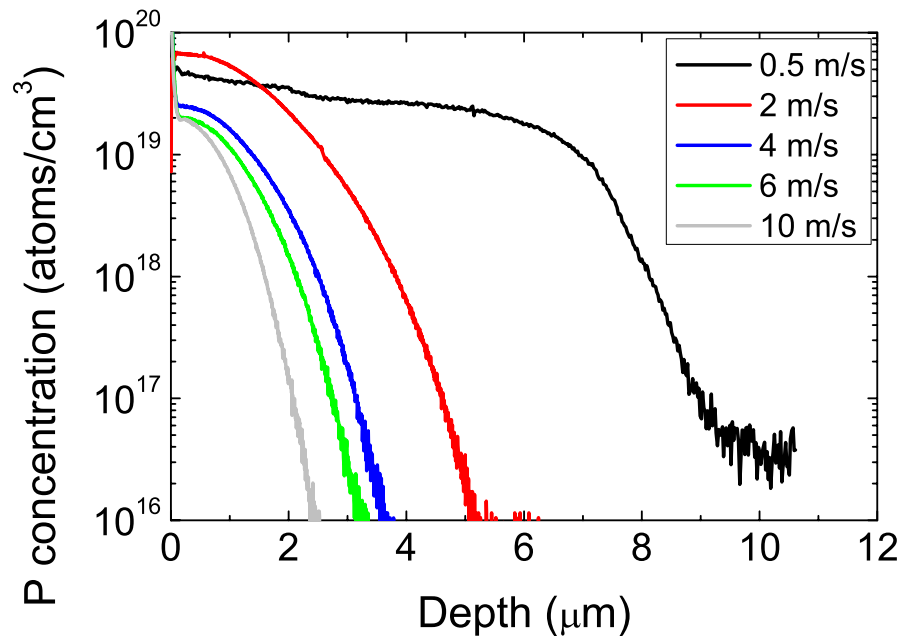
- Dopant profiles in laser doped region aren't always uniform
 - Depends on z , D , t

$$C_{(z,t)} = \frac{Q}{\sqrt{\pi Dt}} e^{-\frac{z^2}{4Dt}}$$



SIMS Profiles of Laser Doped Regions

- CW laser doped regions appear Gaussian for processing speeds of 2 m/s and above
- Characteristic kink for 0.5 m/s profile
- Similar kink for Q-CW laser at 2 m/s
- Artefacts due to multiple laser passes/pulses?

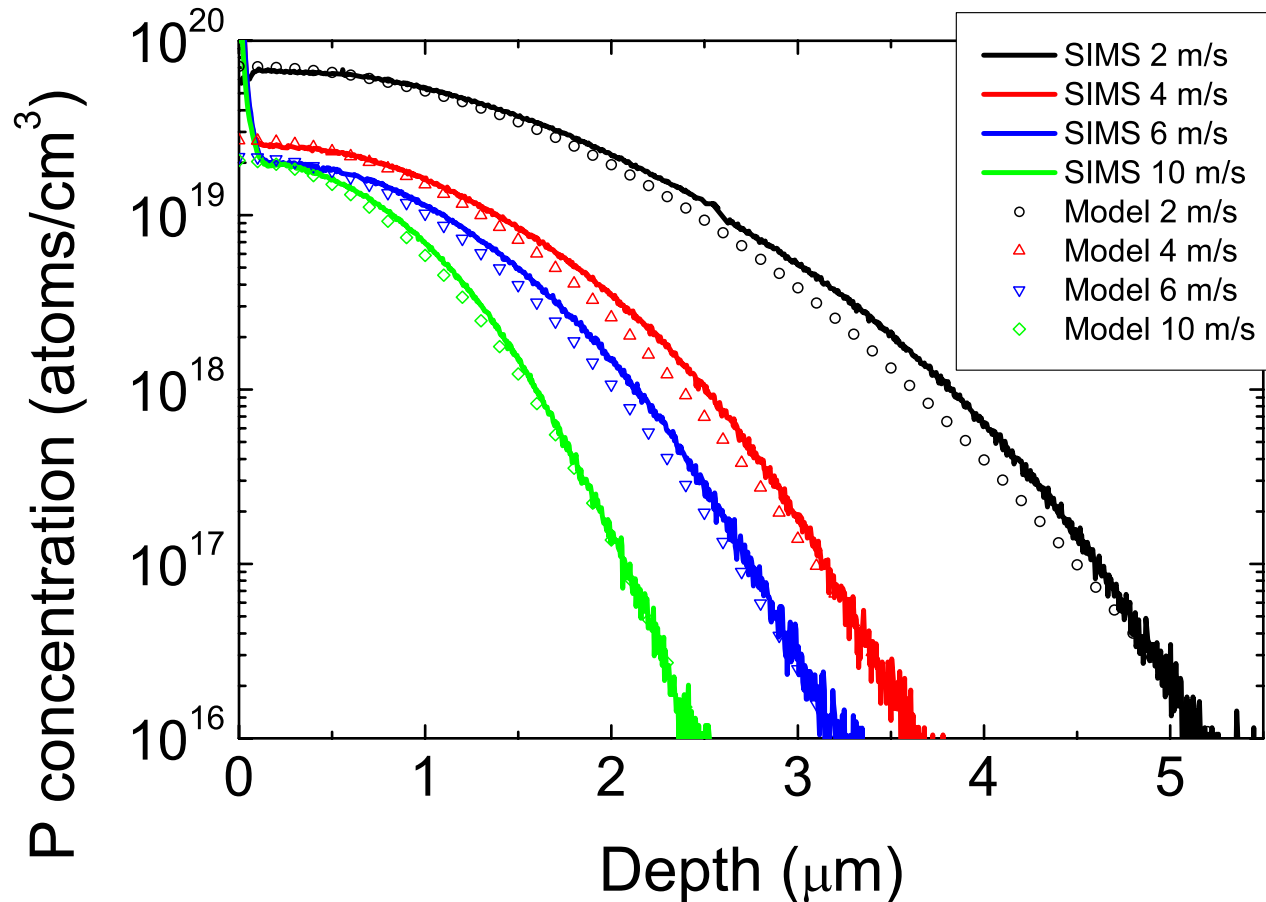


Modelling Diffusion Profiles



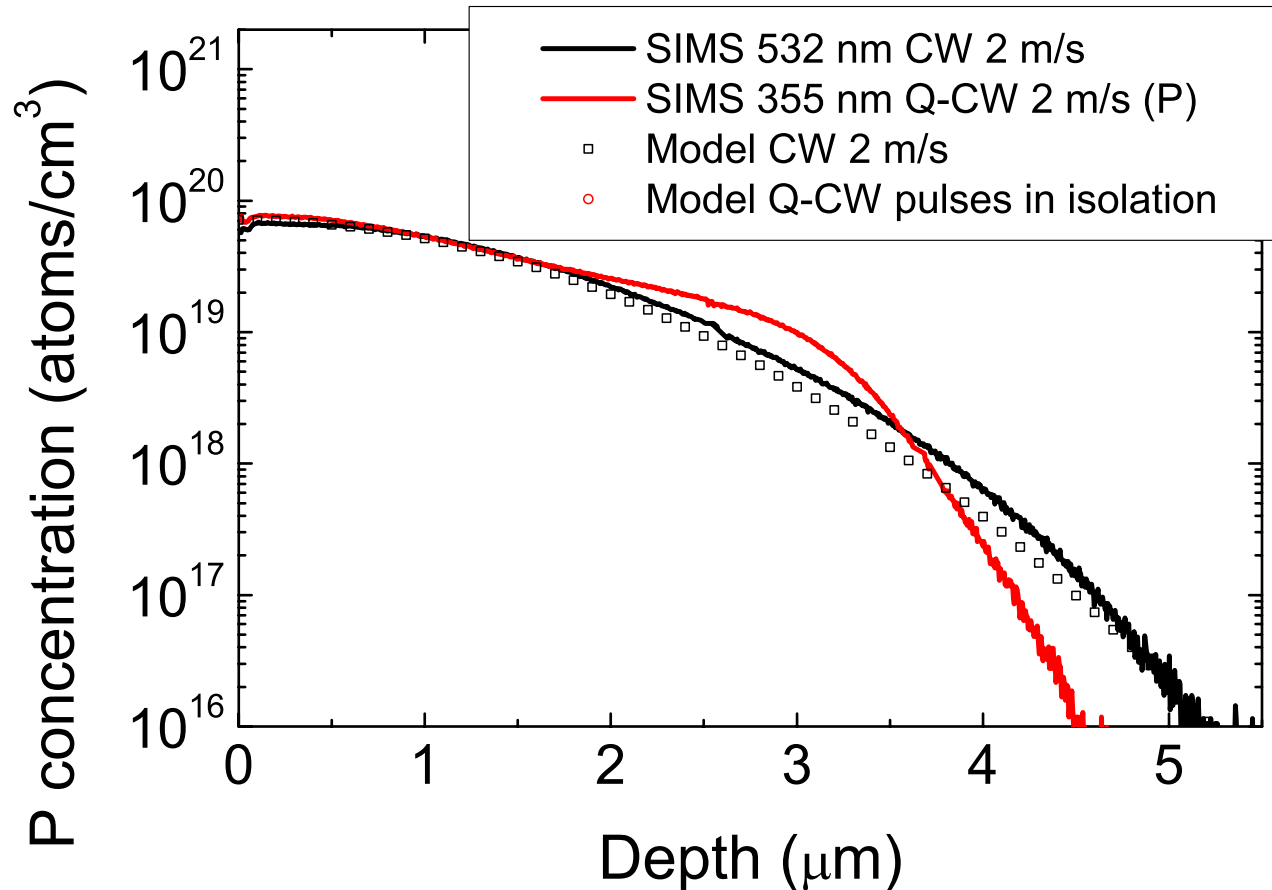
SIMS Profiles of Laser Doped Regions

- Gaussian diffusion theory closely matches profile
 - Discrepancy in intermediate depths
- Silicon remains molten for Q-CW lasers



SIMS Profiles of Laser Doped Regions

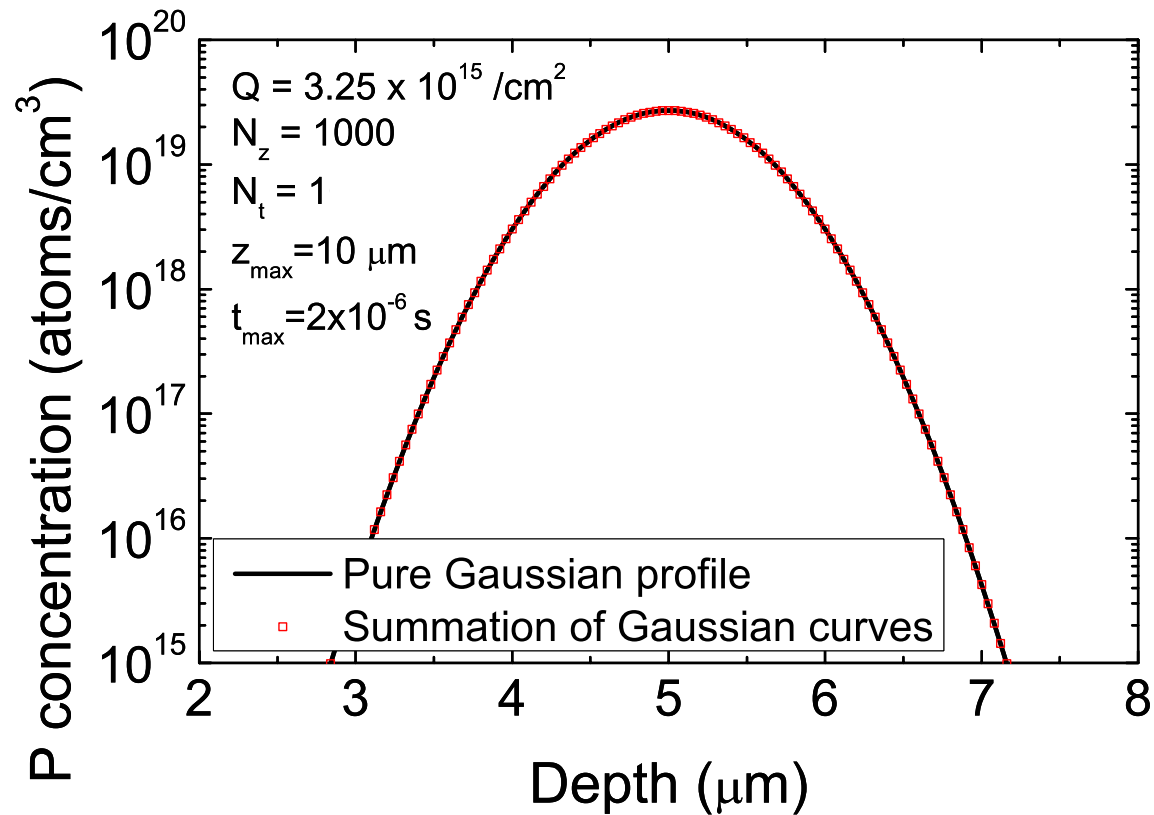
- Gaussian diffusion theory closely matches profile
 - Discrepancy in intermediate depths
- Silicon remains molten for Q-CW lasers



Gaussian Model in the Molten Region

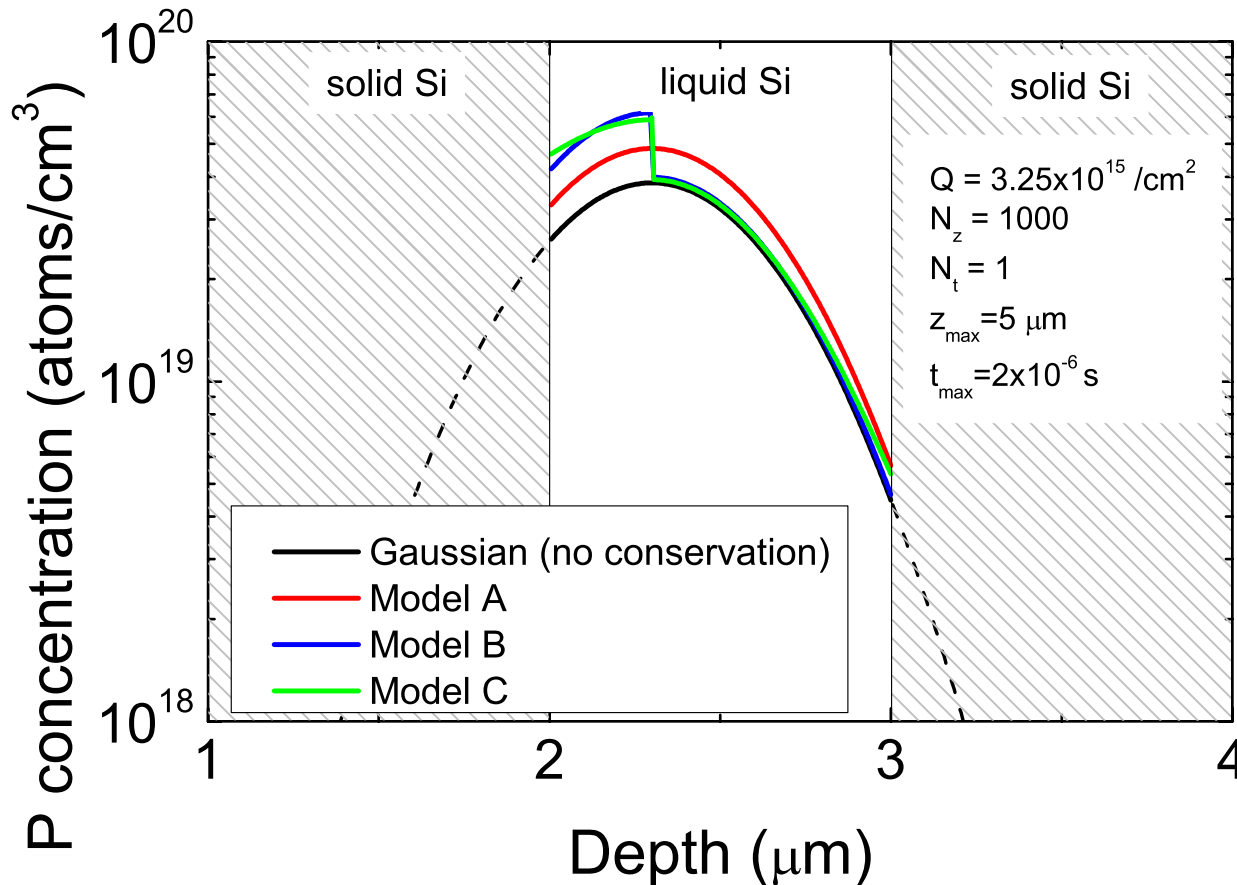
- Single time-step 2 μs , single Gaussian profile seeded from $z=5 \mu\text{m}$
- 1000 time-steps, seed Gaussian profile from each depth (z_k) at each time-step (t_j)

$$\delta C_{(k,z,t_j)} = \frac{C_{(z_k,t_j)} \Delta z}{2\sqrt{\pi D \Delta t}} e^{-\frac{(z-z_k)^2}{4D\Delta t}}$$
$$C_{(z_i,t_{j+1})} = \sum_{k=1}^{N_z} \delta C_{(k,z_i,t_j)}$$



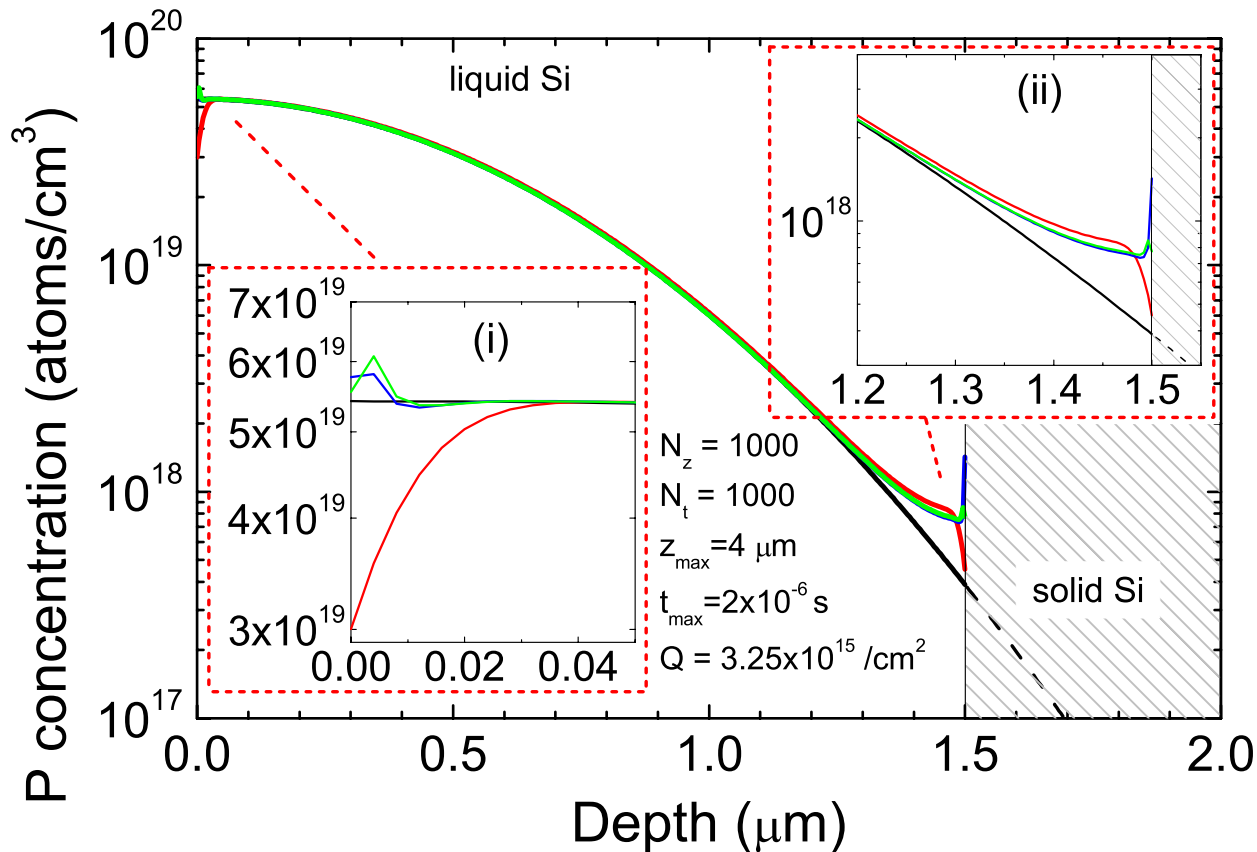
Influence of the Solid/Liquid Interface

- Presence of a solid/liquid interface changes the dopant profile
 - Build up of dopants at solid/liquid interface



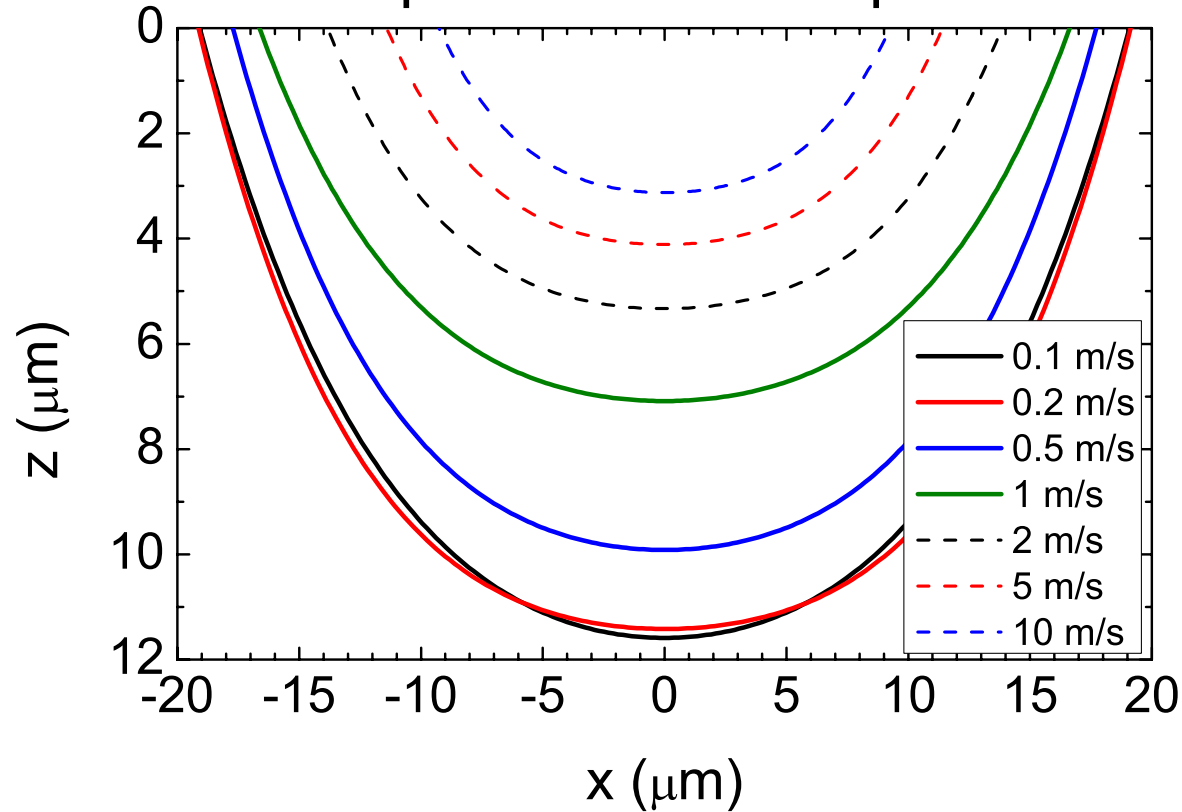
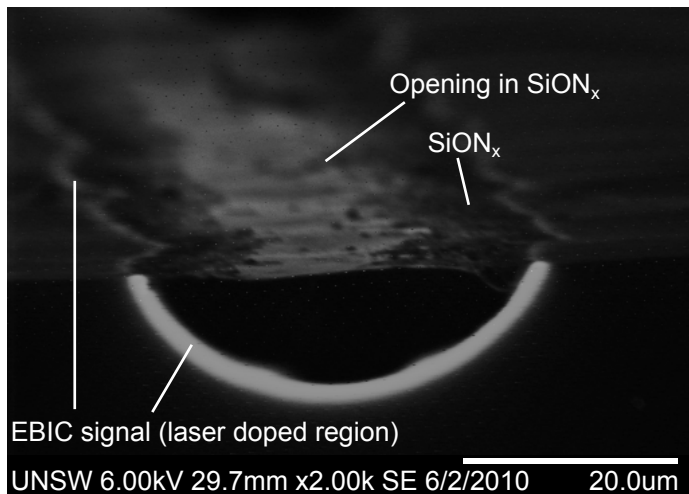
Influence of the Solid/Liquid Interface

- Presence of a solid/liquid interface changes the dopant profile
 - Build up of dopants at solid/liquid interface



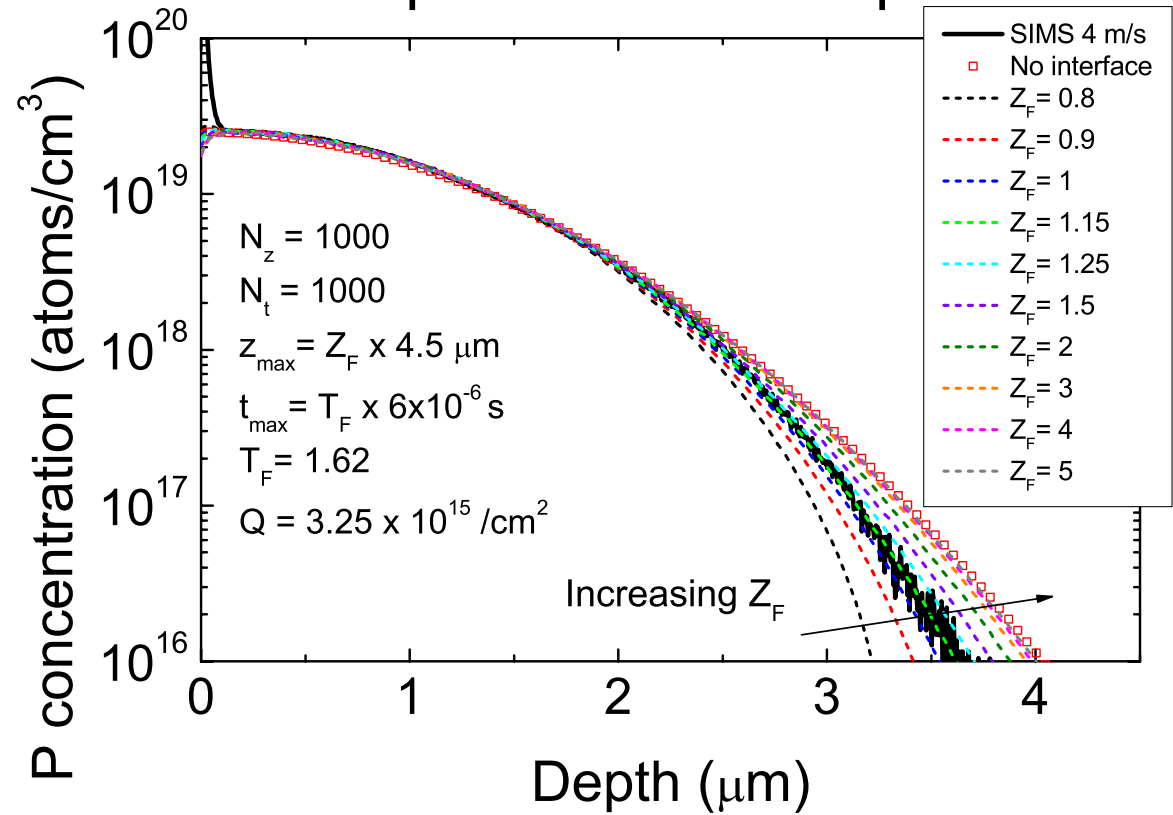
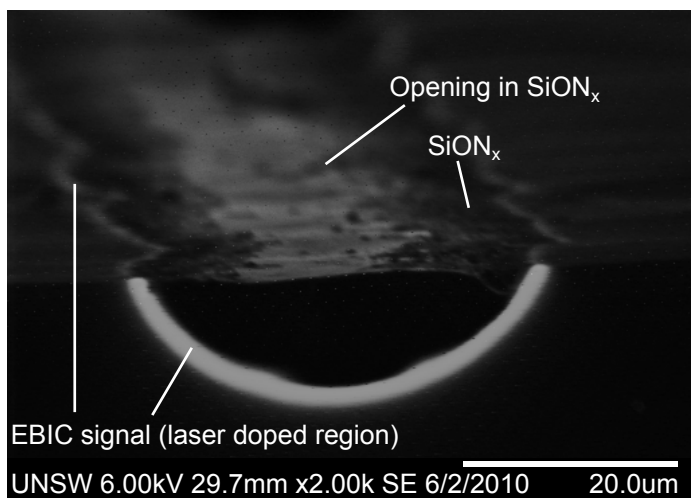
A Time Dependent Solid/Liquid Interface

- $Z_M \sim f(x) \rightarrow f(t)$
- Modify cross sectional dopant profile by depth factor (Z_F) and time dilation factor (T_F) $\rightarrow Z_M = Z_F f(t/T_F)$
- Clear influence of position of solid/liquid interface on profile



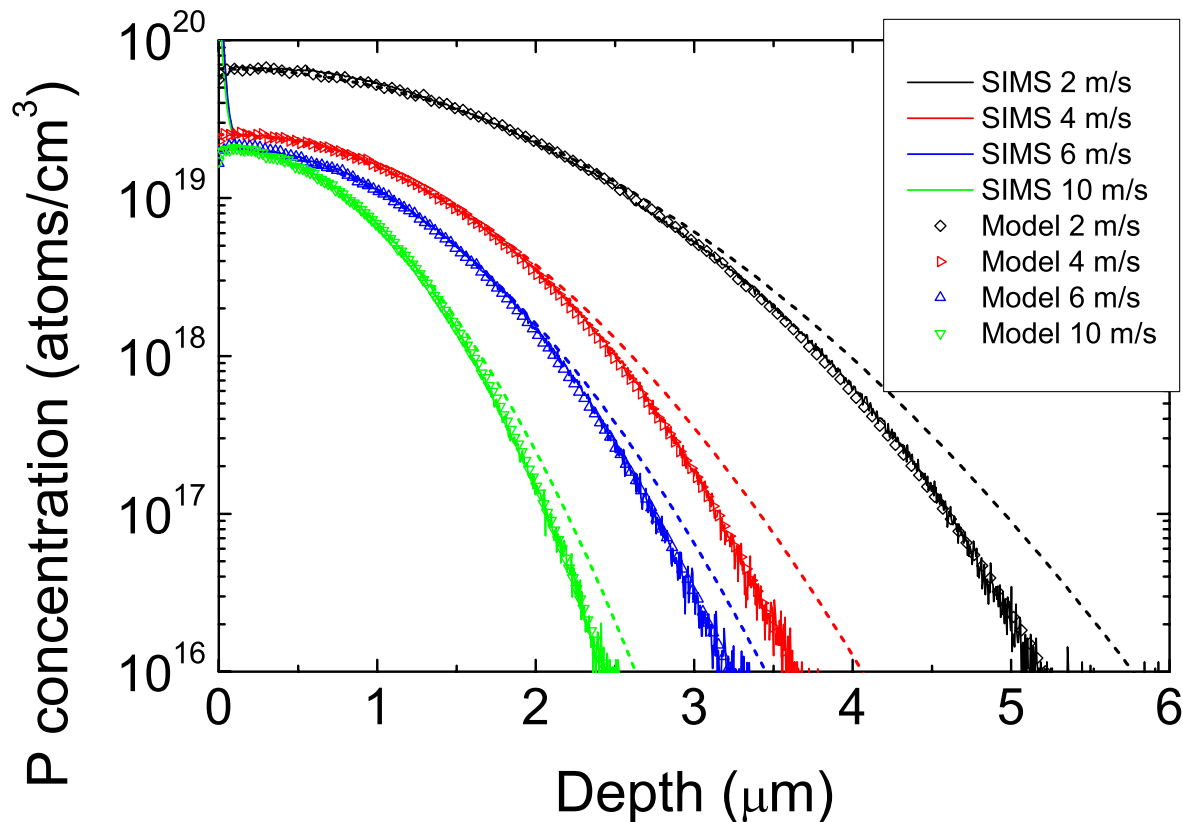
A Time Dependent Solid/Liquid Interface

- $Z_M \sim f(x) \rightarrow f(t)$
- Modify cross sectional dopant profile by depth factor (Z_F) and time dilation factor (T_F) $\rightarrow Z_M = Z_F f(t/T_F)$
- Clear influence of position of solid/liquid interface on profile



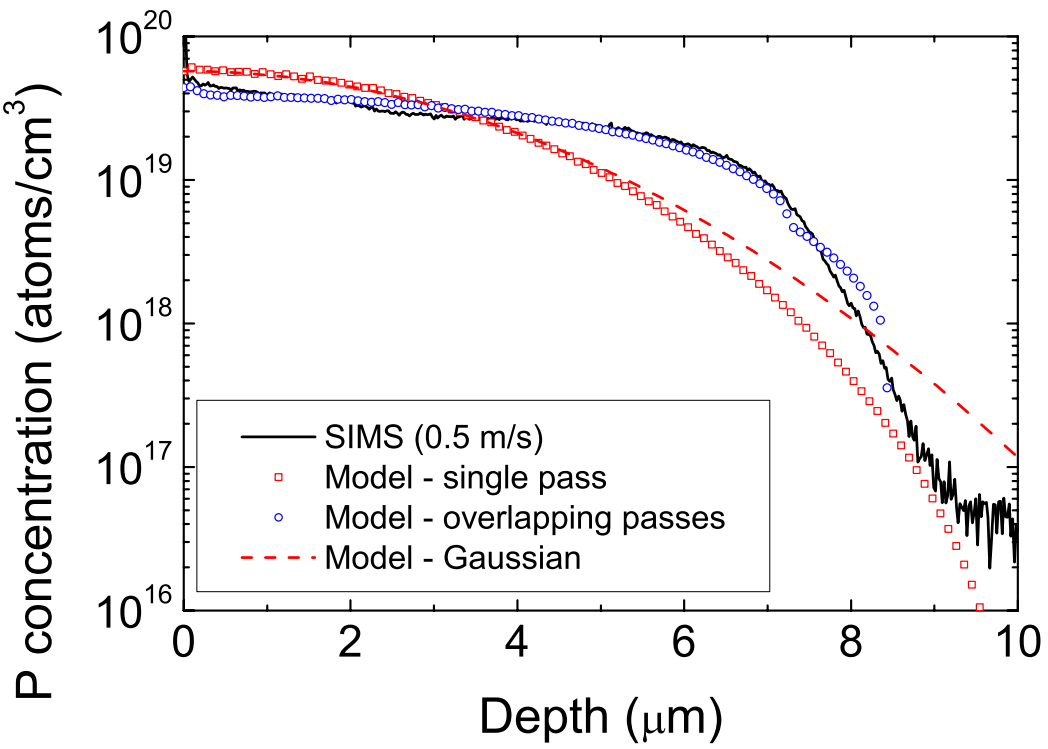
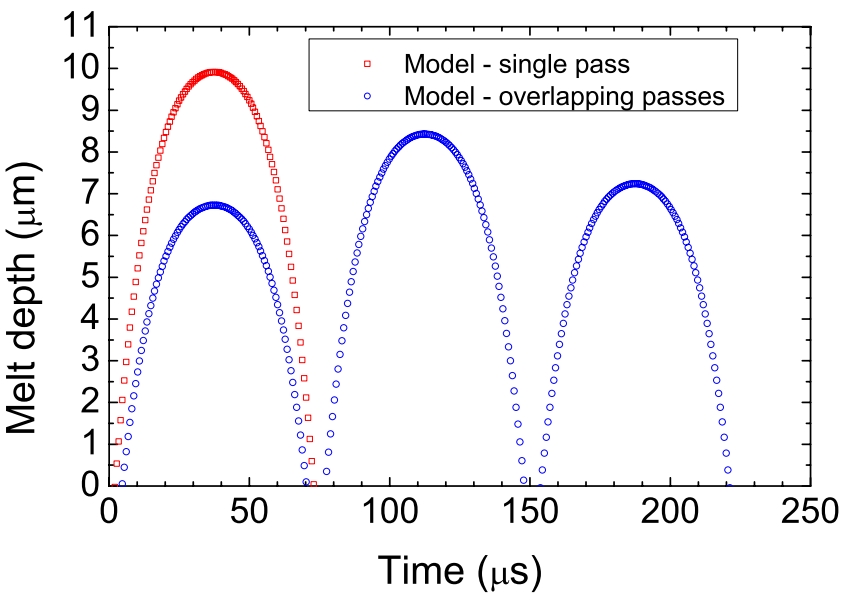
A Time Dependent Solid/Liquid Interface

- Influence of the solid/liquid interface can accurately describe the SIMS profiles
- Doesn't work for 0.5 m/s → multiple passes?



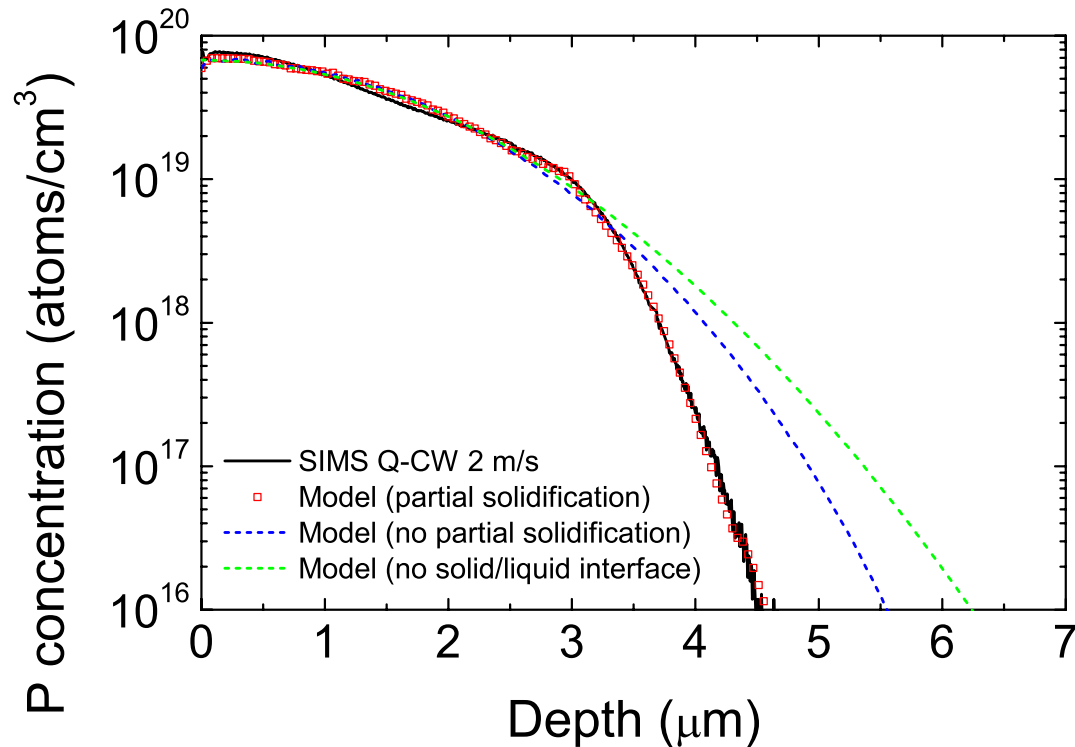
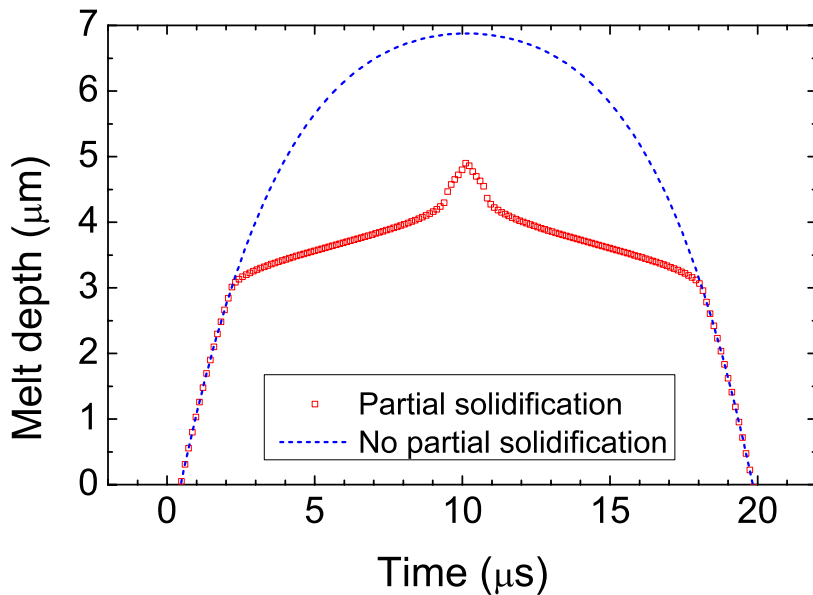
A Time Dependent Solid/Liquid Interface

- Influence of the solid/liquid interface can accurately describe the SIMS profiles
- Doesn't work for 0.5 m/s → multiple passes?



Partial Solidification for Q-CW Laser Doping

- Q-CW laser doped regions can be represented by a single effective pulse with a reduced melt depth
 - Represent a partial solidification between successive pulses (80 MHz) for the larger depths

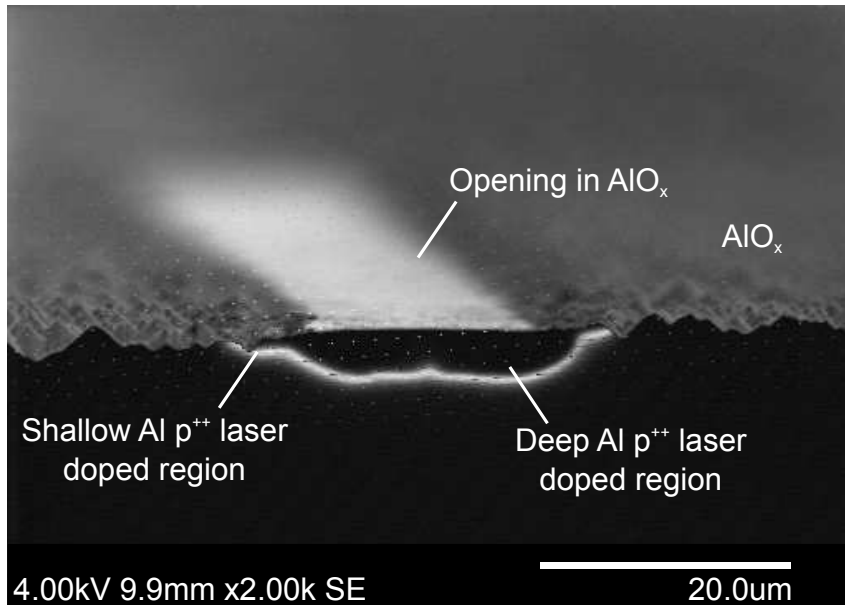


Laser Doping from Al_2O_3 Layers

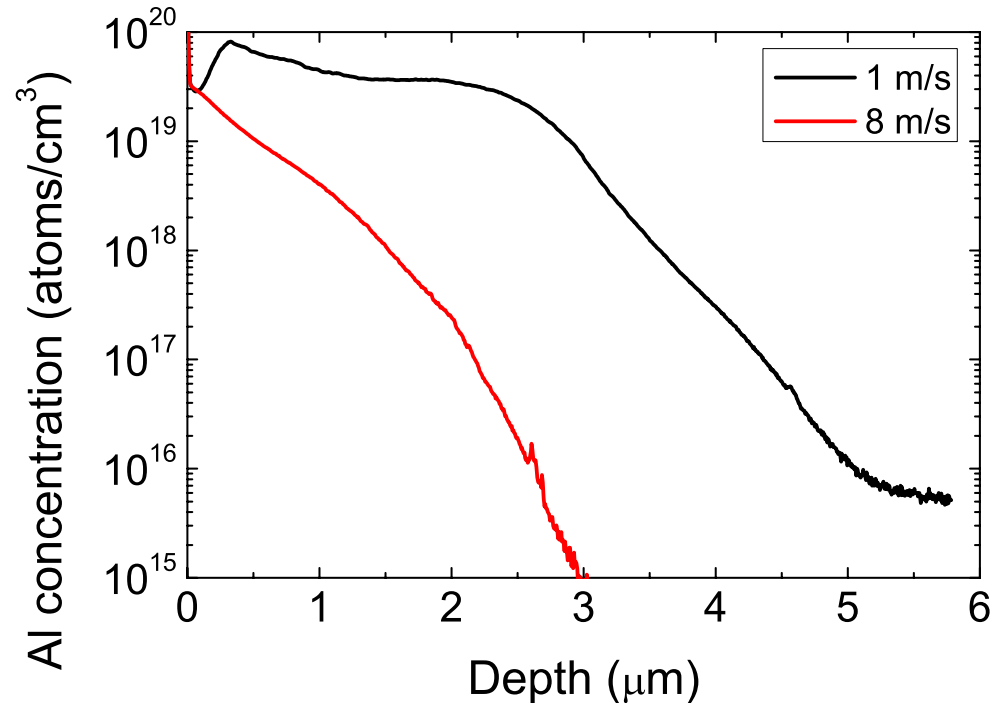


Effective Doping from Al₂O₃ Layers

- Effective doping from Al₂O₃ layers
 - Solid state diffusion in peripheral regions?
- Up to 35% utilisation of Al atoms from Al₂O₃ layers (10 nm)
- Much higher doping concentrations than conventional BSF (~2x10¹⁸ /cm³)

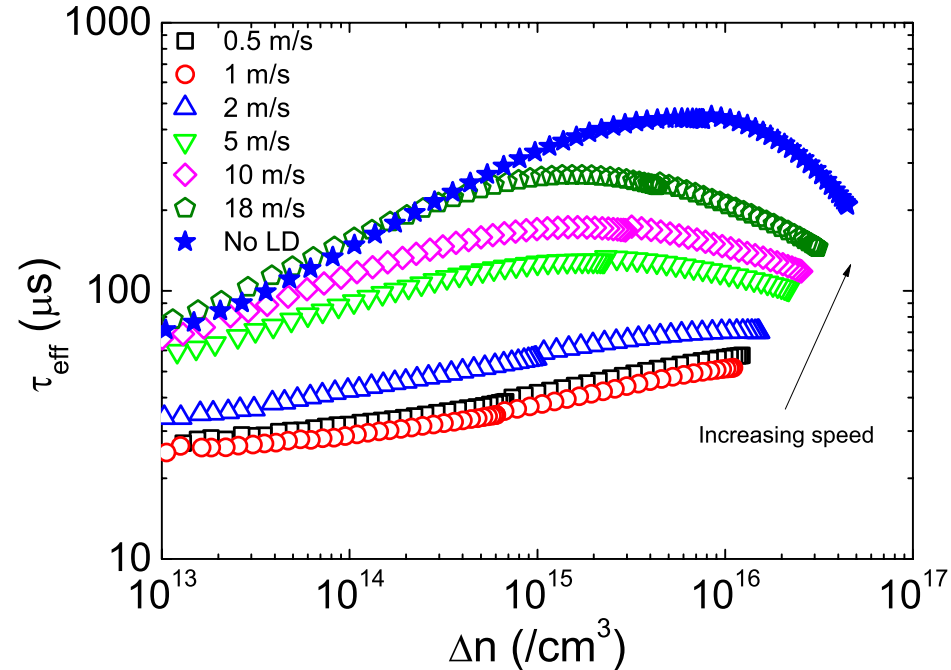
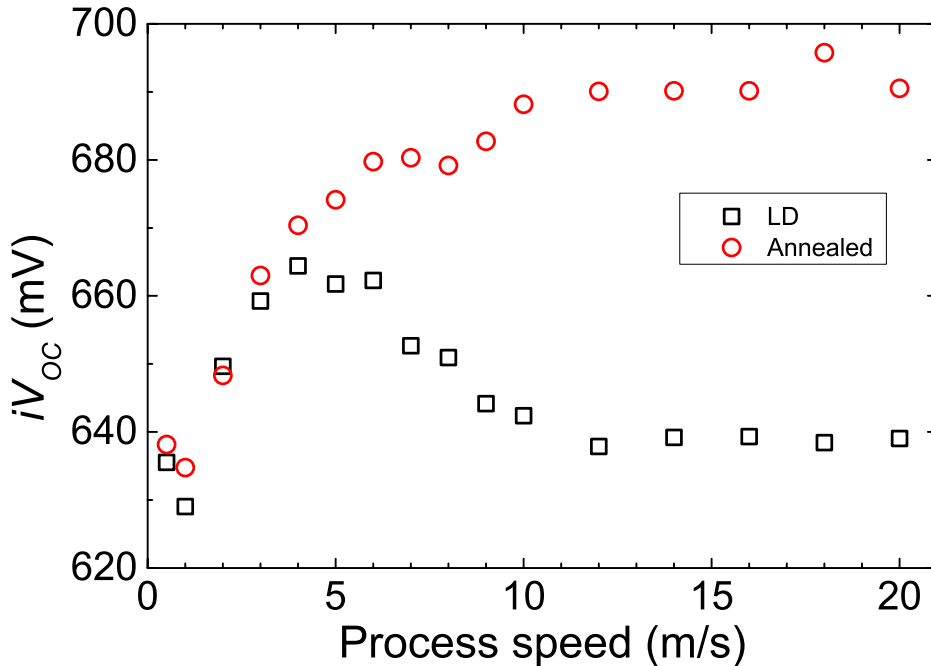
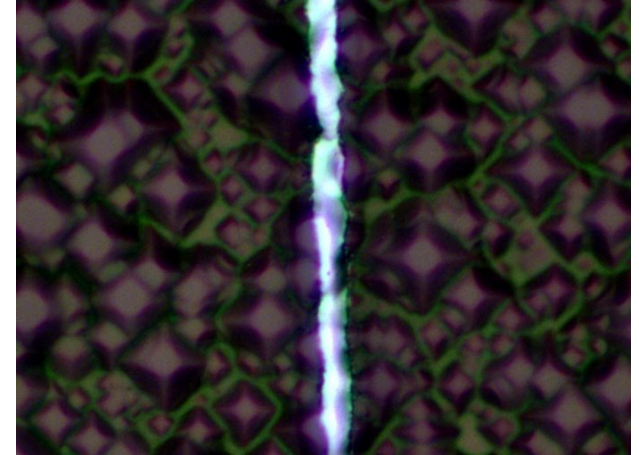


Al₂O₃ LD on a textured surface (2 m/s)



Contact formation by Al_2O_3 Laser Doping

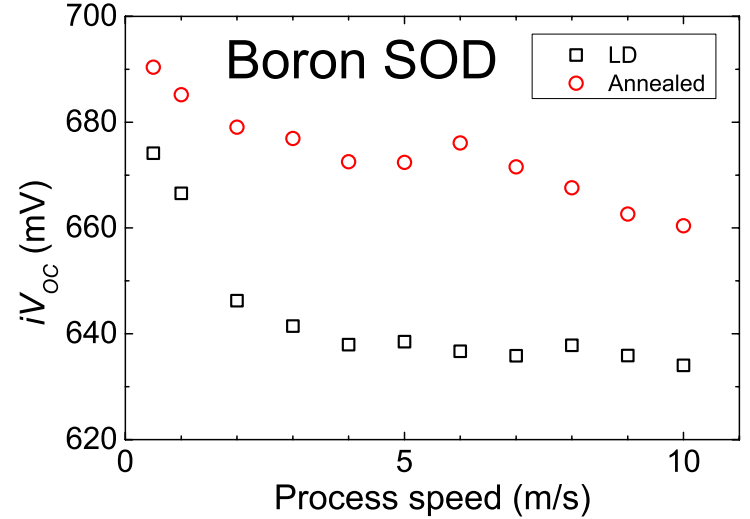
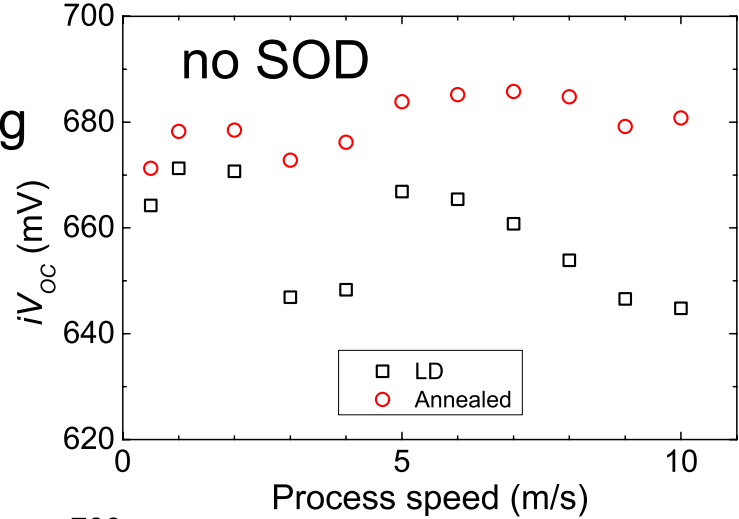
- Stack of $\sim 5 \mu\text{m}$ opening (10 m/s through 10nm Al_2O_3 / 50nm SiO_x)
- Increasing $iV_{\text{OC}} / \tau_{\text{eff}}$ with increasing speed
 - Avoidance of bulk defects



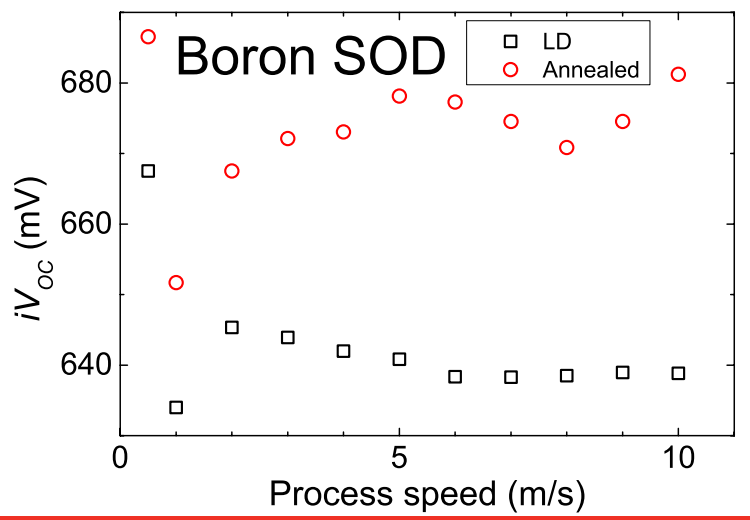
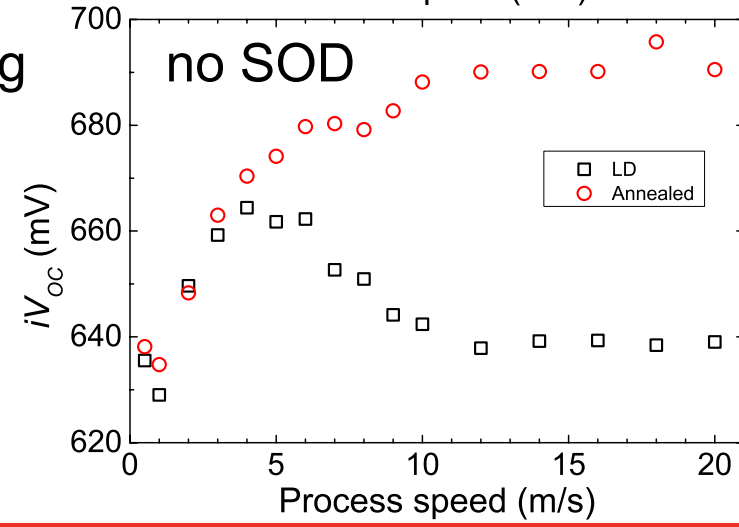
Dependence of Dielectric Layers / SOD

- Results dependent on dielectric stack / presence of additional dopants

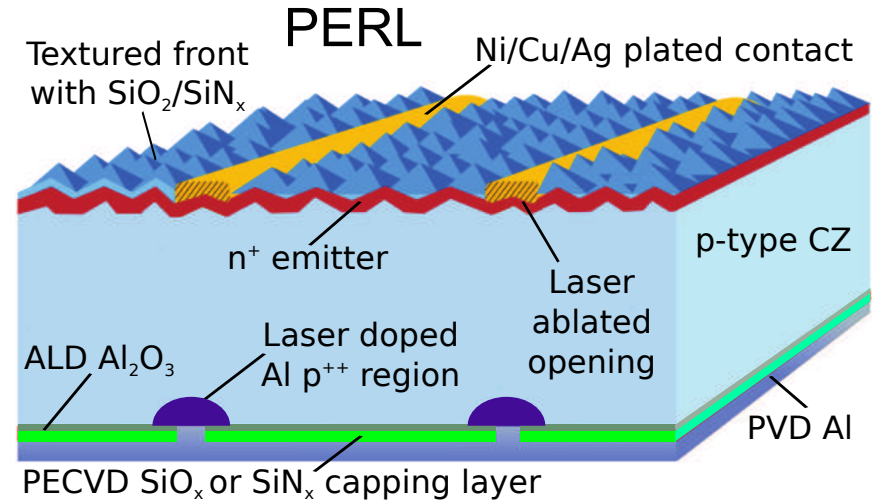
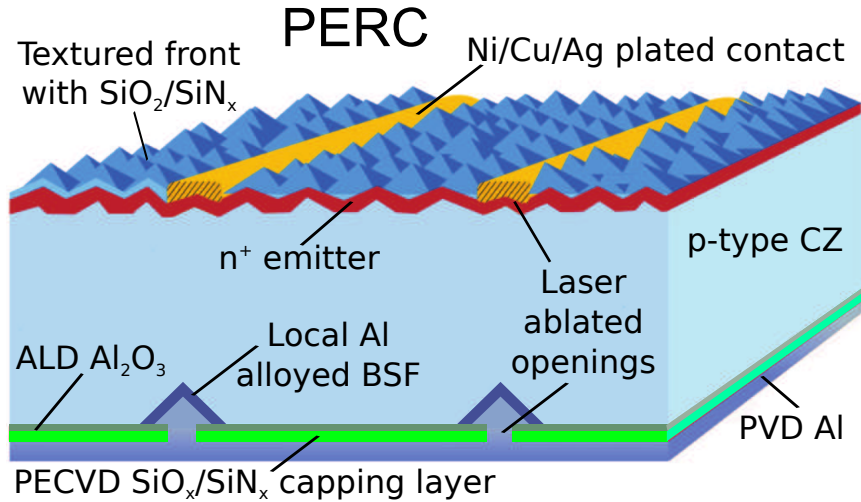
SiN_x capping



SiO_x capping



Cell Fabrication with Al₂O₃ Laser Doping



Process	J _{SC} (mA/cm ²)	V _{OC} (mV)	FF (%)	pFF (%)	η (%)
PERC (Av)	39.4 ± 0.2	659 ± 3	79.7 ± 0.3	82.0 ± 0.2	20.4 ± 0.2
PERL (Av)	39.5 ± 0.1	653 ± 3	79.2 ± 0.4	82.4 ± 0.1	20.4 ± 0.2
PERL* (best)	39.4	657	79.9	-	20.7

- Incorporation of LDSE front → + 0.4% efficiency (21.1%)
- Incorporation of improved hydrogenation
→ increase V_{OC} > 680 mV, J_{SC} ~ 40 mA/cm² (21.8%)

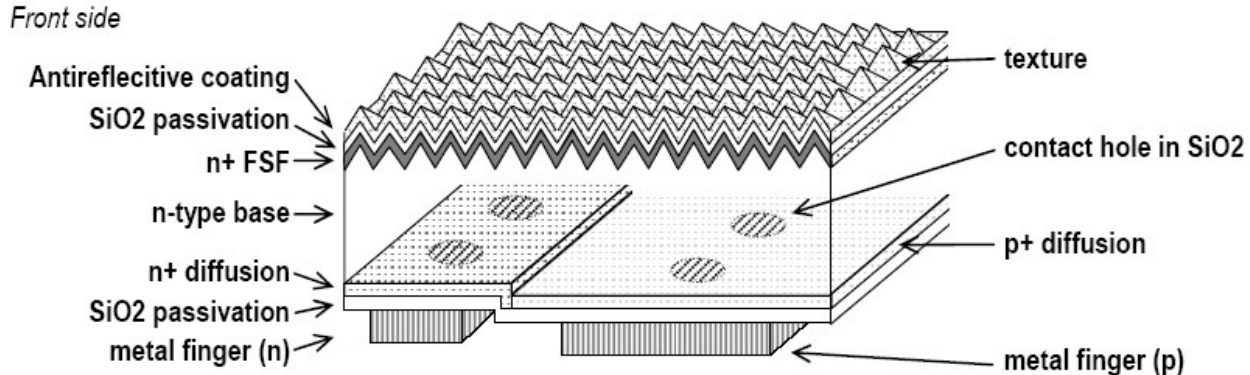
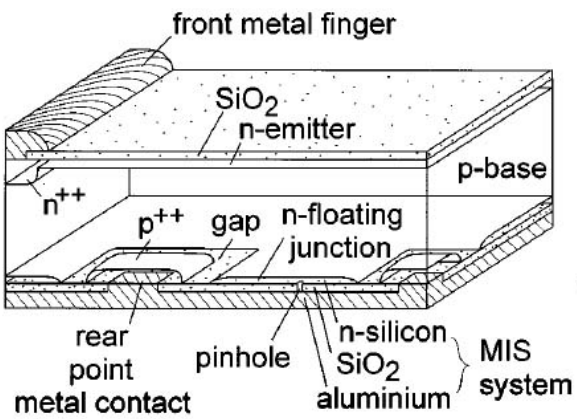


Contacting Buried Layers in Silicon Solar Cells

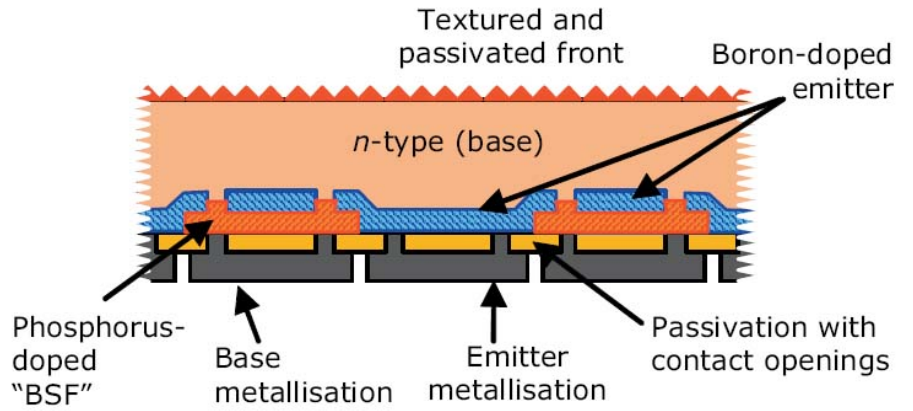
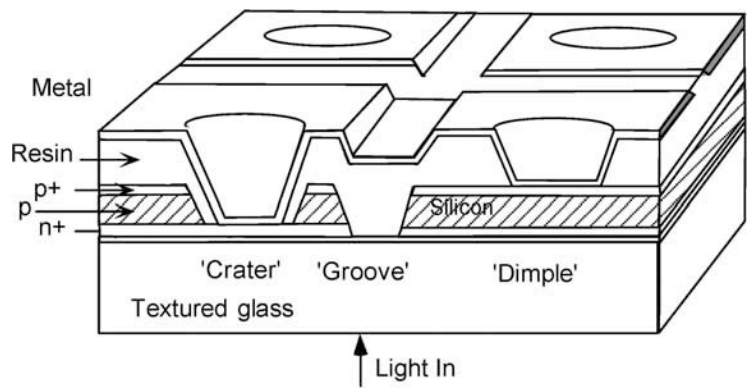


The Need to Contact Buried Layers

- Contacting buried layers in silicon solar cells requires complex processing
 - Masking/etching
 - Multiple diffusions



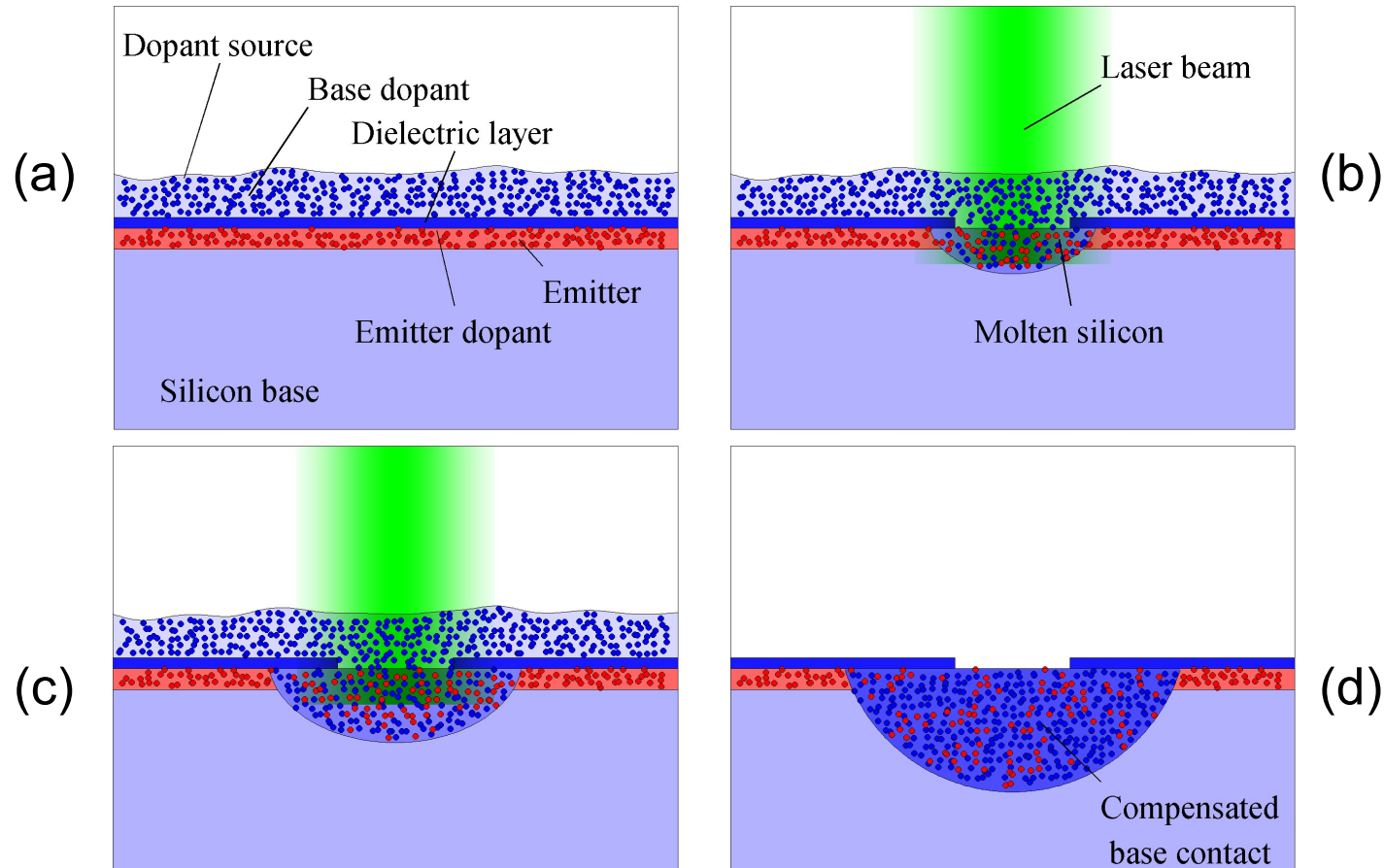
Rear side



P. Altermatt et al. Journal of Applied Physics , Vol. 80, pp. 3574 (1996). N. Harder et al. physica status solidi RRL, Vol. 2, No. 4, pp. 148 (2008). W. P. Mulligan et al. Proc. of the 19th EU PVSEC, pp 387 (2004). M. Green et al. Solar Energy , Vol. 77, No. 6, pp. 857 (2004).

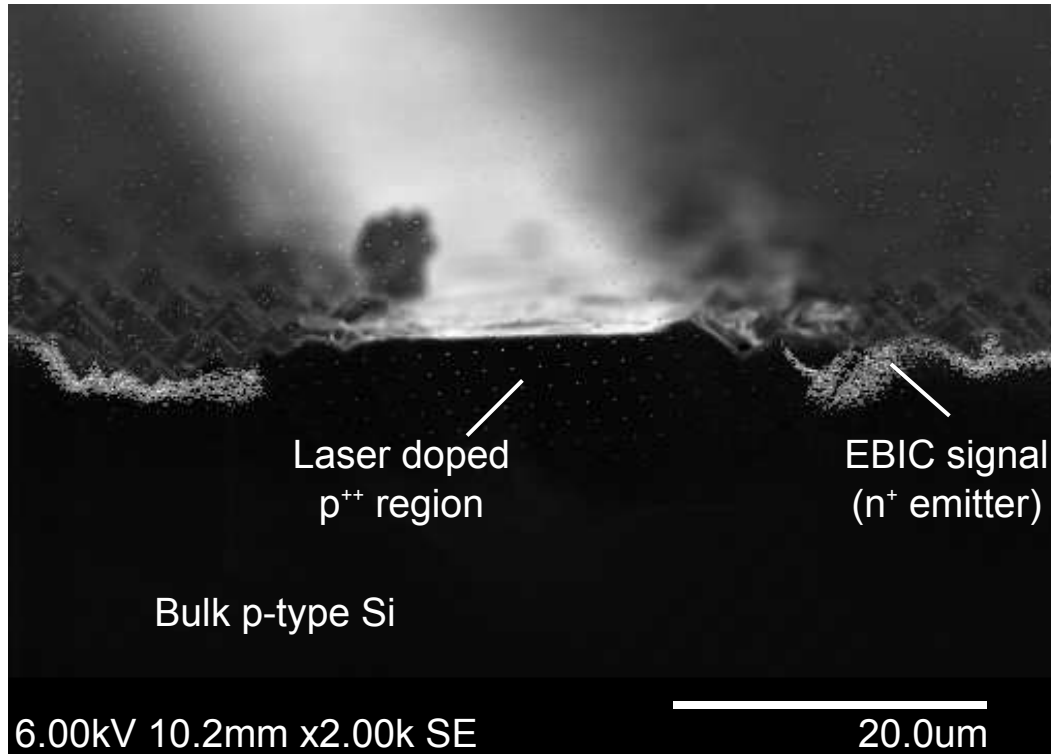
Laser Doping for Contact Buried Layers

- Single self-aligned process to contact layer under the surface
 - No masking/etching
 - Single conventional thermal diffusion



Contacting Buried Layers for IBC Cells

- Successful demonstration of penetrating through an industrial phosphorus emitter ($120 \Omega/\text{sq}$) with boron laser doping
 - No masking/etching
 - IBC solar cells with single thermal diffusion and two alignment steps
- 14.5% efficiency in initial trials [Chan 2012]

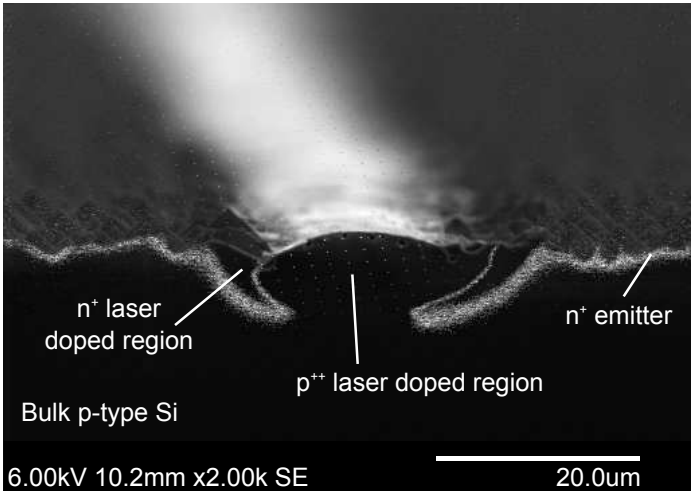


p-type LD on a textured phosphorus emitter
(0.2 m/s)

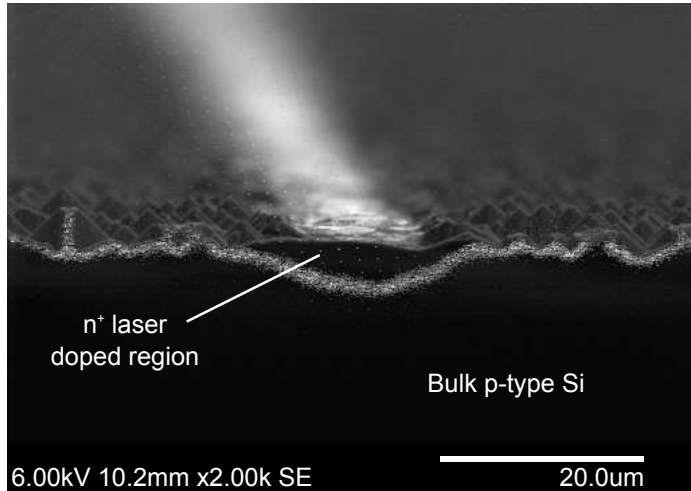
Transistor formation

- Changing process conditions / emitter profile can result in transistor formation

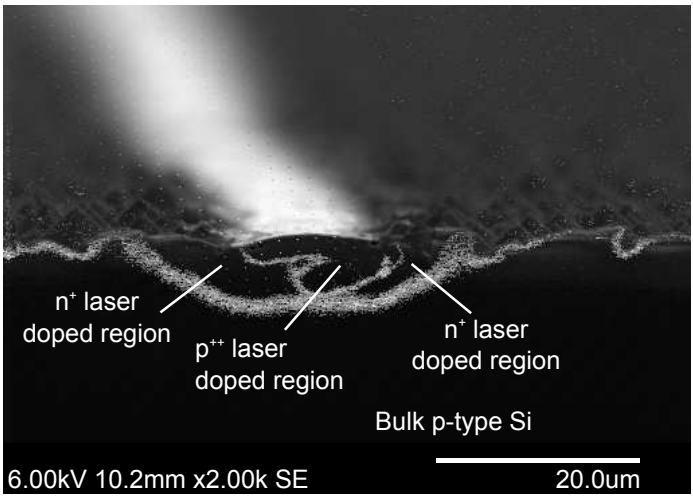
1 m/s



5 m/s

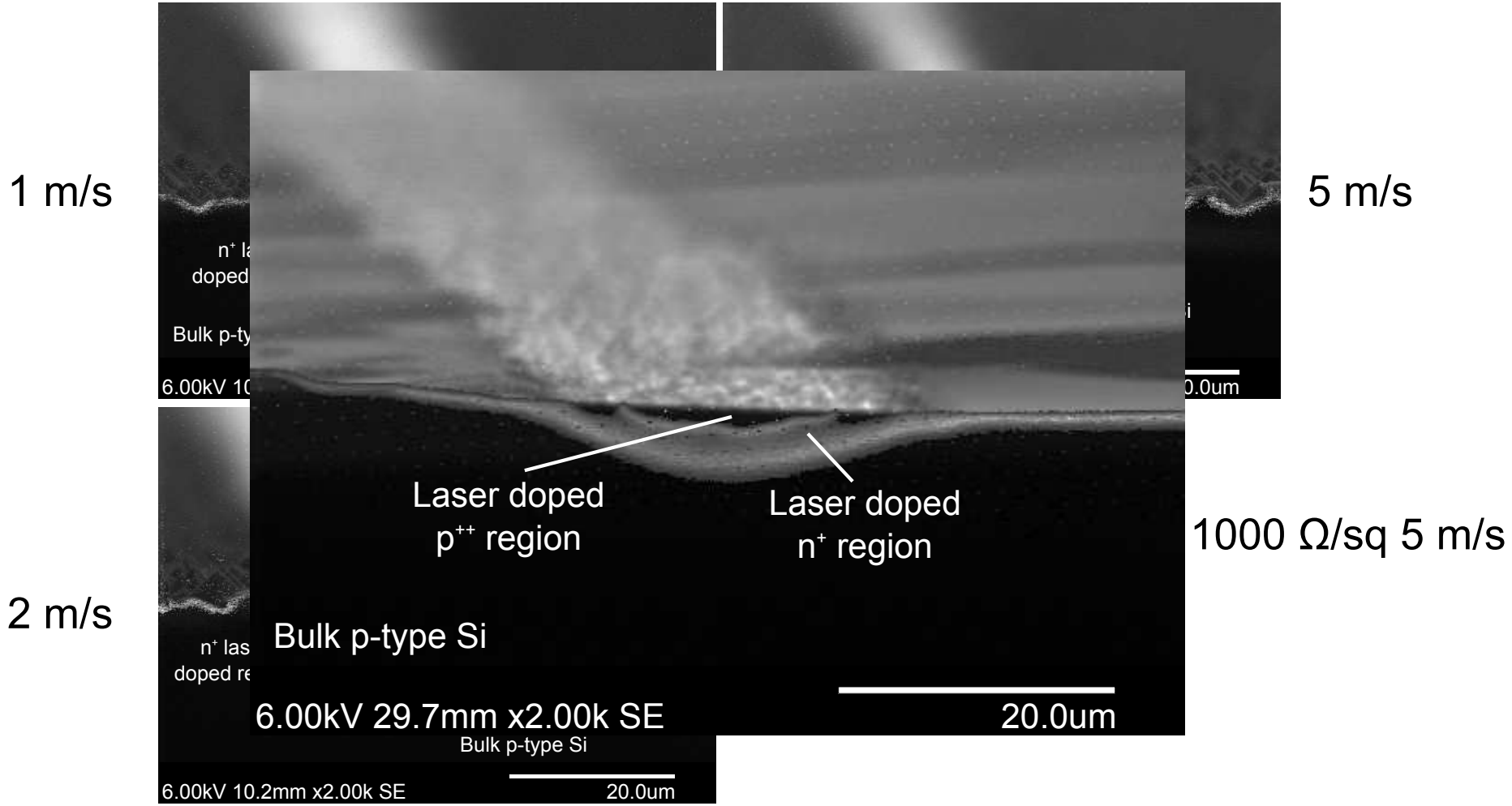


2 m/s



Transistor formation

- Changing process conditions / emitter profile can result in transistor formation

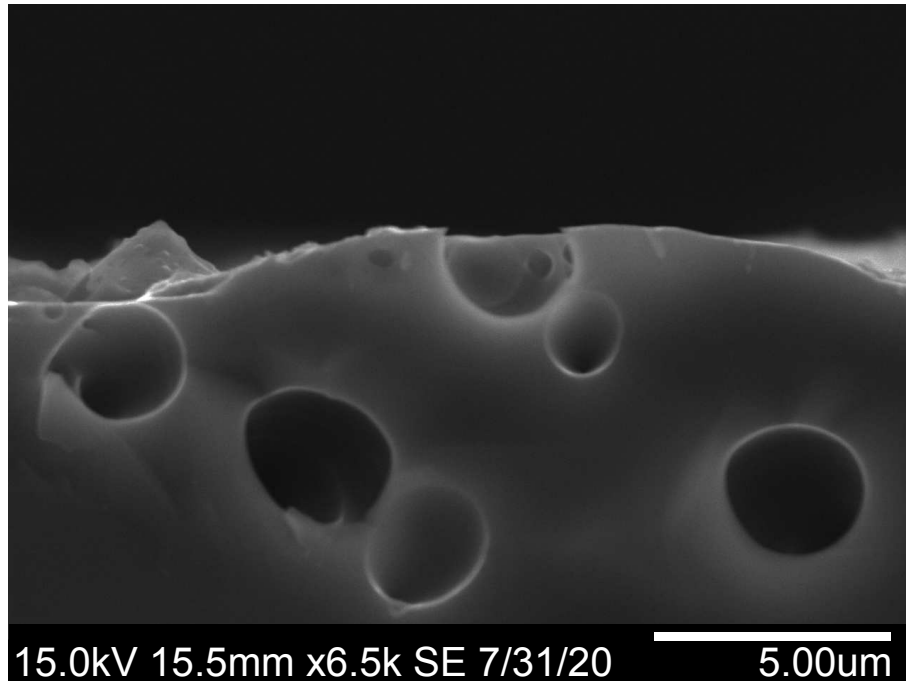


Passivation of Laser-Induced Defects

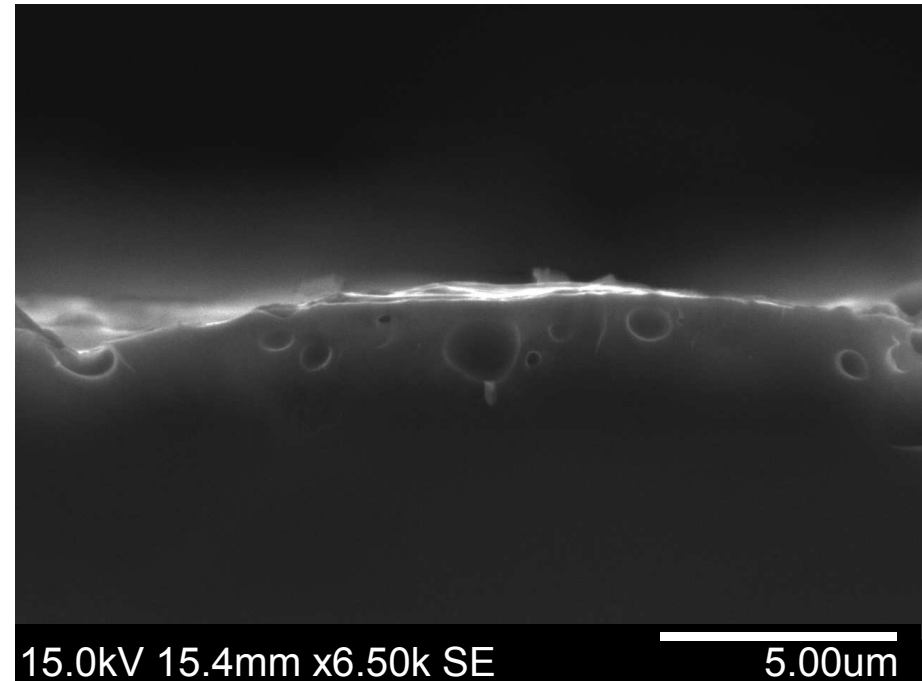


Void Formation during CW Laser Doping

- Voids can form with diameters $> 4 \mu\text{m}$
- Dependent on speed / SOD / dielectric layer
 - Most prevalent at 0.5 m/s



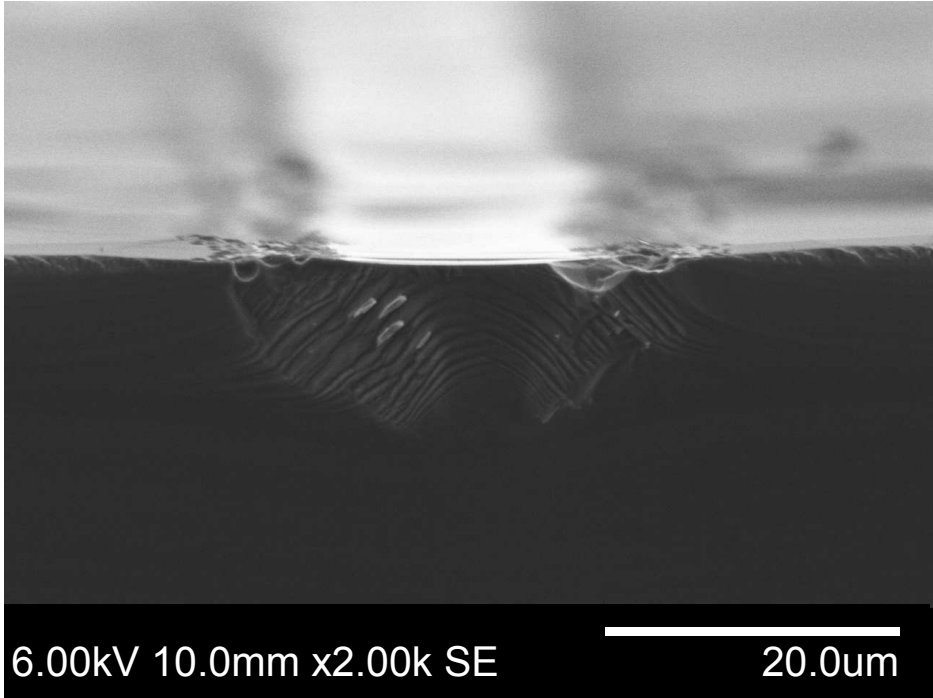
0.5 m/s



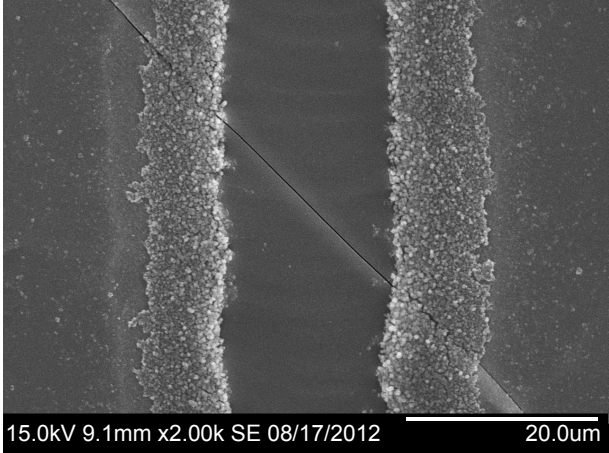
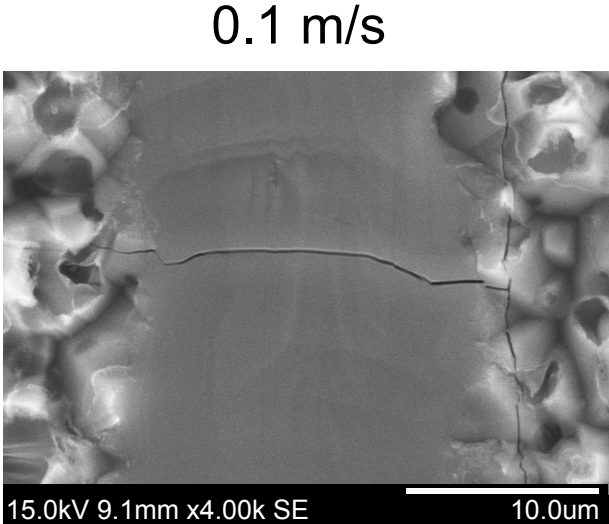
1 m/s

Crystallographic Defect Formation

- Crystallographic defects are evident for processing speeds < 0.5 m/s



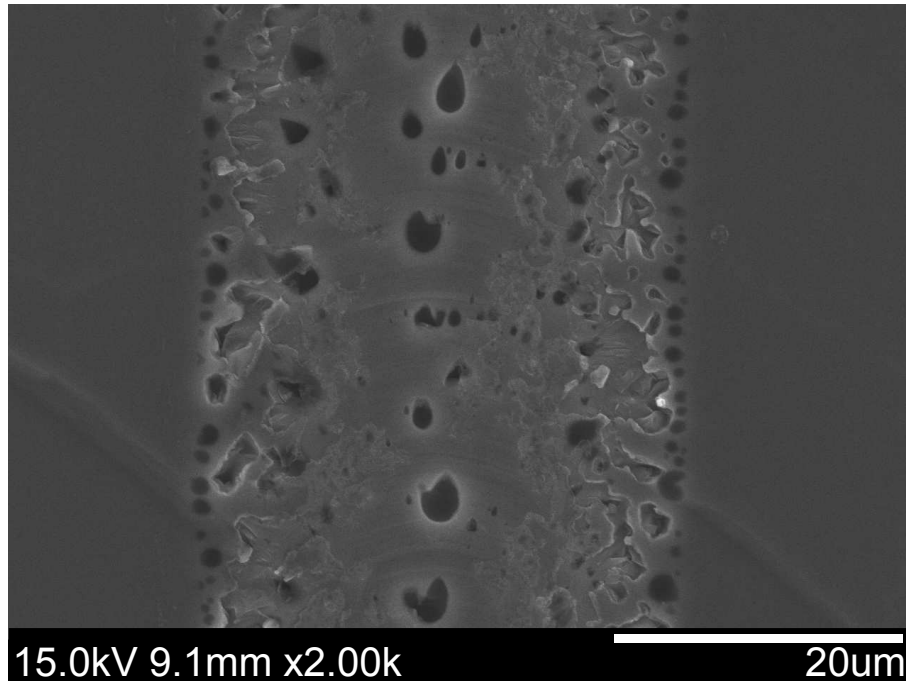
0.1 m/s



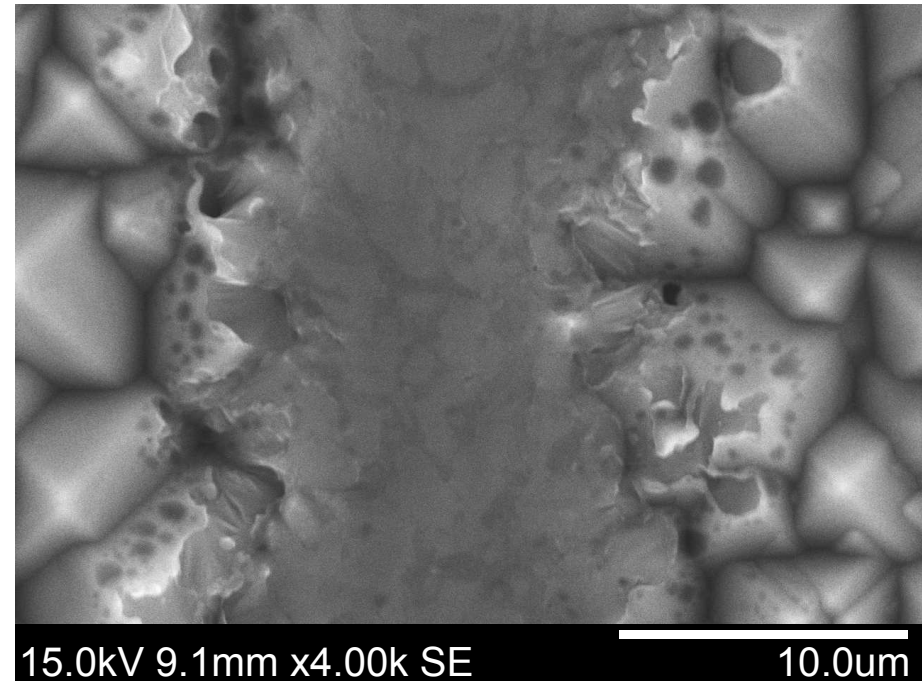
0.01 m/s

Pinhole Formation in Dielectrics

- Pinhole formation in dielectrics beyond opened region
 - Require doping to protect against recombination



0.5 m/s

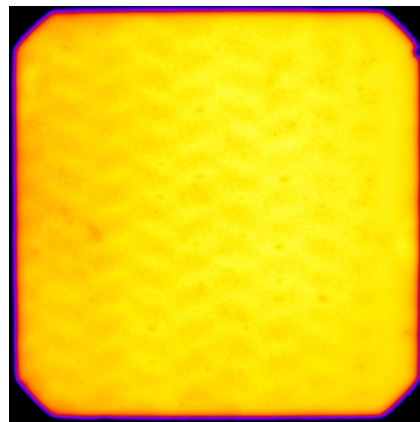


5 m/s

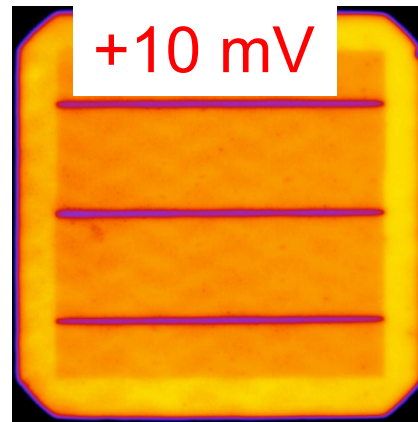
Passivation of Laser-Induced Defects

- Laser processing can introduce bulk/surface defects
- H a key to passivating laser-induced defects
 - Annealing 1-2 min @ 400°C utilising H in the the wafer
- Ni sinter can also be used for H passivation

Process	J_{sc} (mA/cm ²)	V_{oc} (mV)	FF (%)	pFF (%)	η (%)
No anneal (Av)	37.78	627.4	77.42	83.2	18.35
Anneal (Av)	37.69	636.7	77.97	83.6	18.71

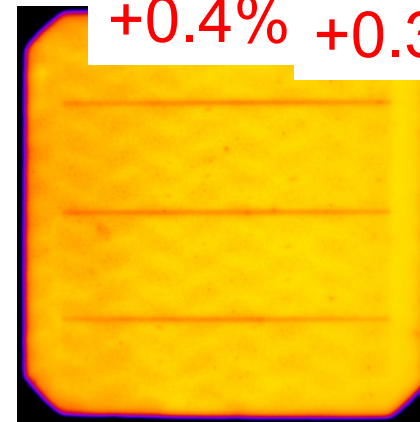


Al-BSF



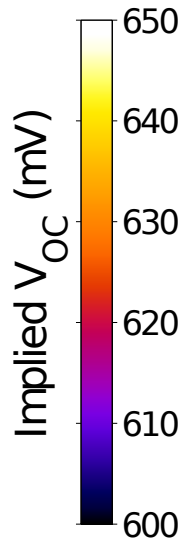
+10 mV

LD



+0.4% +0.35%

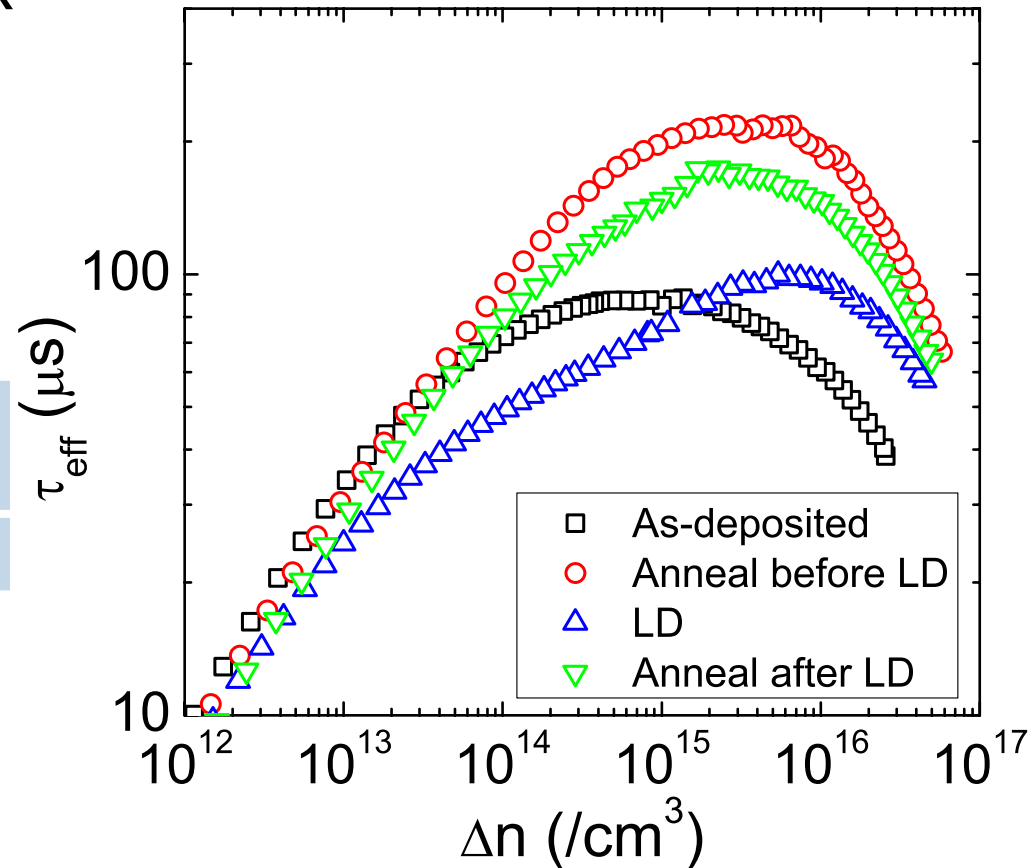
Anneal



Bulk and Surface Damage from LD

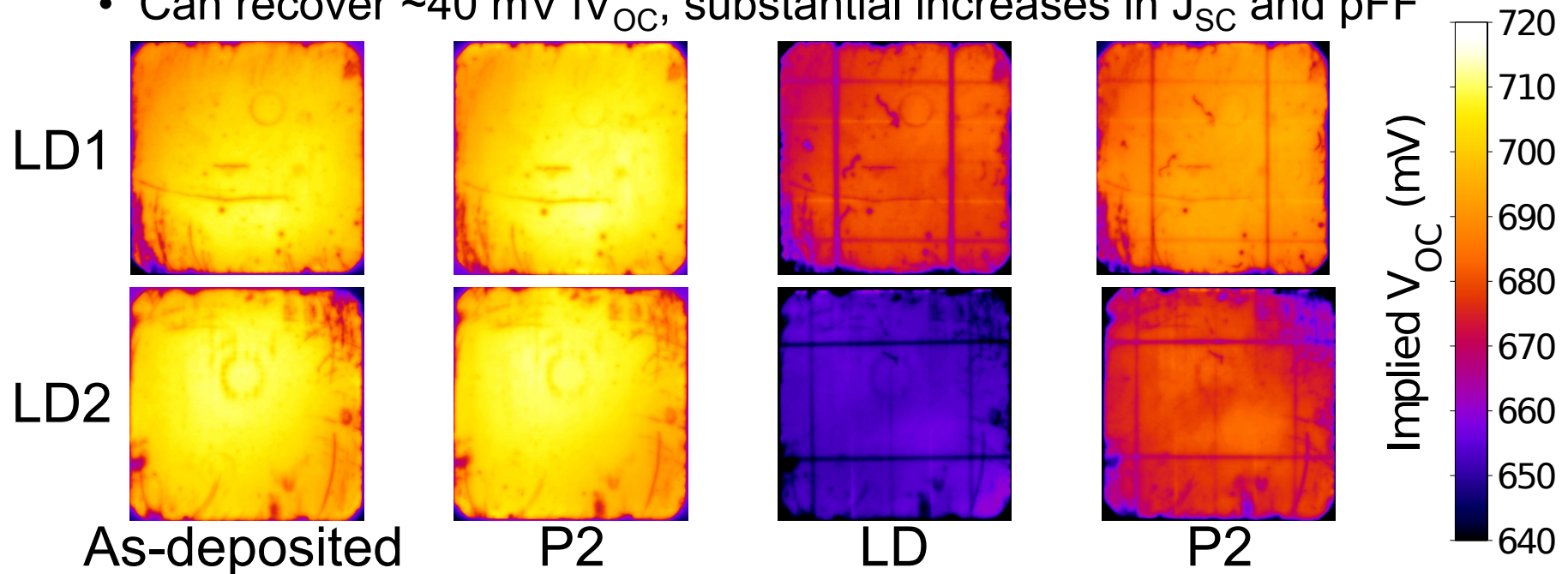
- Test structure $n^+/p/n^+$ passivated by SiON:H
- H passivation (400 °C in N_2) reduces J_{0d} and increases τ_{bulk}
- Laser doping damages bulk
- Subsequent anneal passivates laser-induced defects

Process	iV_{oc} (mV)	J_{0d} (fA/cm ²)	τ_{bulk} (μ s)
As-dep	648	140	129



High Voltage Test Structures

- Modification of PECVD process to enhance hydrogen passivation (only little extra improvement from P2)
 - Enhanced H-radical incorporation into SiN and Si
- Laser processing generates defects
- H passivation important for laser induced defects
 - Up to 1% absolute increase in efficiency observed so far
 - Can recover ~ 40 mV iV_{OC} , substantial increases in J_{SC} and pFF

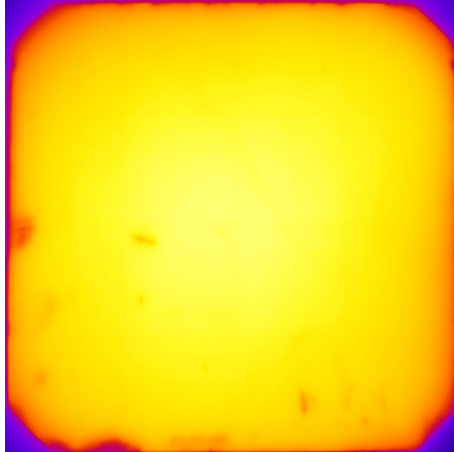


Passivation of Laser-Induced Defects for n-PERT

- Similar effect for passivation of laser-induced defects on n-PERT solar cells
- 15 mV improvement through passivation of laser-induced defects
- iV_{OC} still limited by busbar region (20 mV lower)

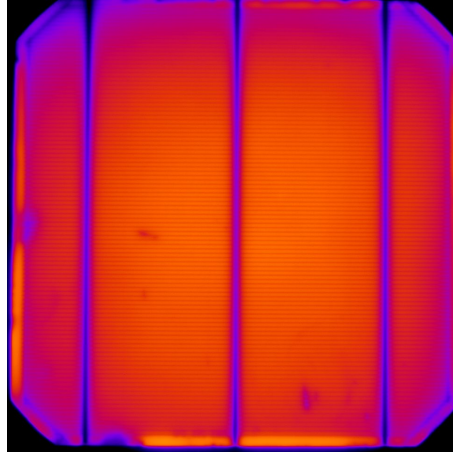


710 mV



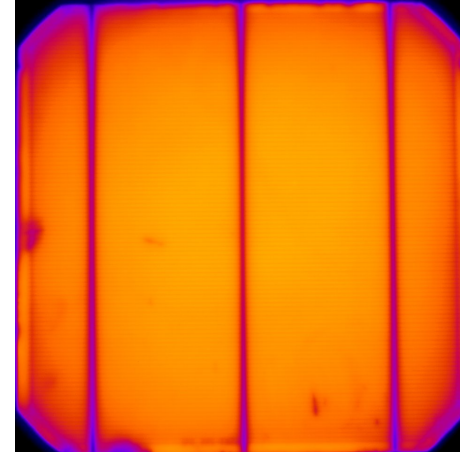
Alneal

670 mV

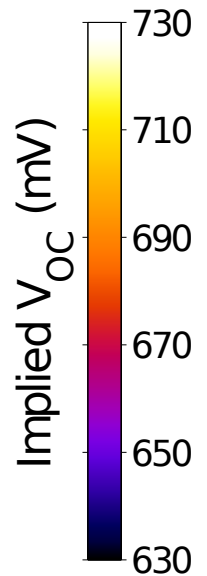


LD

685 mV

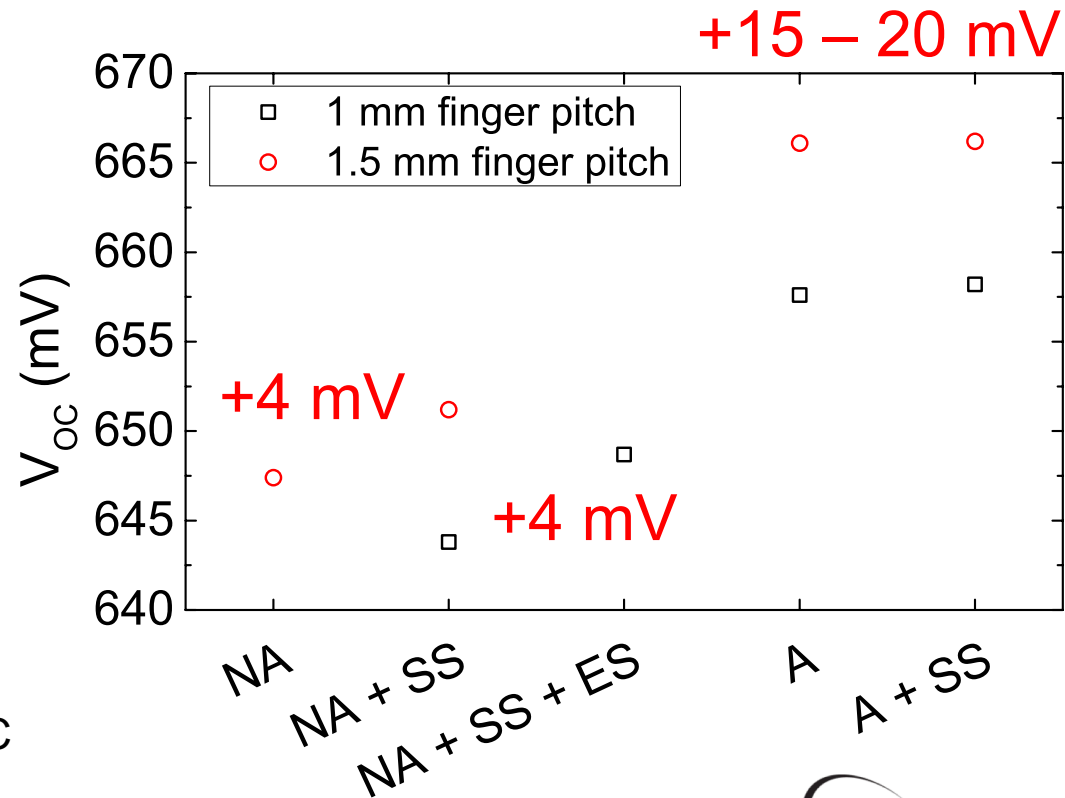


Anneal



Improvement in passivation for n-PERT

- Standard IMEC Ni sintering process (SS) reasonably ineffective for hydrogen passivation of laser-induced defects
- Performing an extra sinter at elevated temperature (ES) more effective for passivation
- Annealing at 450 °C for 3 mins in O₂ ambient (A) prior to plating substantially improves V_{OC}
- Passivation stable during subsequent SS process



Efficiency enhancement for n-PERT through passivation of laser-induced defects

- 0.7% efficiency increase through hydrogen passivation of laser-induced defects
- Further efficiency increases through improved hydrogen passivation of other defects in the device



+0.3 mA/cm²

+15 mV

+0.2%

+0.7%

Process	J _{sc} (mA/cm ²)	V _{oc} (mV)	FF (%)	pFF (%)	η (%)
No anneal 1.5 mm (Av)	39.19	648.4	77.97	82.18	19.81
Anneal 1.5 mm (Av)	39.48	664.1	78.34	82.42	20.54
No anneal 1.0 mm (Av)	38.23	643.2	79.56	82.13	19.56
Anneal 1.0 mm (Av)	38.75	657.1	79.53	82.26	20.25



Thank you for your attention

brett.hallam@unsw.edu.au

